Instrumentation Development, Measurement and Performance Evaluation of Environmental Technologies

Quarterly Technical Progress Report
for the period
April 1, 2000 - June 30, 2000

Dr. John Plodinec, Principal Investigator

Report No. 40395R08

Prepared for the U.S. Department of Energy
Agreement No. DE-FC26-98FT40395

Diagnostic Instrumentation and Analysis Laboratory
Mississippi State University
205 Research Boulevard
Starkville, Mississippi 39759-9734

dial@dial.msstate.edu
www.msstate.edu/Dept/DIAL

Notice

This report was prepared as an account of work sponsored by an agency of the United States Government. Neither the United States Government nor any agency thereof, nor any of their employees, makes any warranty, express or implied, or assumes any legal liability or responsibility for the accuracy, completeness, or usefulness of any information, apparatus, product or process disclosed or represents that its use would not infringe privately-owned rights. Reference herein to any specific commercial product, process, or service by trade name, trademark, manufacturer, or otherwise does not necessarily constitute or imply its endorsement, recommendation, or favoring by the United States Government or any agency thereof. The views and opinions of authors expressed therein do not necessarily state or reflect those of the United States Government or any agency thereof.

Table of Contents

Executive Summary 1

TASK 1 Characterization of Heavy Metals, Radionuclides and Organics in Heterogeneous Media 6

Volatile Organic Compound Monitoring Using Diode Lasers 6
Metal Continuous Emission Monitors (APO-GEM) 11
Sensitive Detection of Toxic Chlorinated Organic Compounds. 14
Isotopically Selective Monitors for Transuranic Elements 17
Laser-induced Breakdown Spectroscopy 26

TASK 2 Environmental Control Device Testing. 32

Performance Enhancement of the Ionizing Wet

Scrubber 32
Testing of a Ceramic Regenerative Heat Storage Device for Dioxin Control and Heat Recovery 34
Transportable Calibration Test Stand for Diagnostic Instrumentation. 38
Evaluation and Performance Enhancement of a Submerged Bed Scrubber. 40

TASK 3 Waste Treatment and D&D Support: Process Monitoring and Control 44

Dioxin and PCB Studies 44
On-line Multi-spectral Imaging of Thermal Treatment Processes. 48
Detection and Possible Mitigation Strategy for Gall Layer in Hanford High Level Waste Melters 51
Imaging Instrumentation Application and Development: Thermal Imaging 54
Imaging Instrumentation Application and Development: Profilometry 57
Saltcake Dissolution 58
Feed Stability and Chemistry: Solids Formation 70

TASK 4 Diagnostic Field Applications Coordination and Testing Support 88

List of Figures

FIGURE 1. Ringdown signal obtained using an infrared-wavelength distributed feedback diode laser 8

FIGURE 2. Response of the infrared ringdown system when a small amount of chlorobenzene is introduced into the cell. 9

FIGURE 3. Schematic diagram of the CRDS setup. 15

FIGURE 4. Cavity ring-down spectrum of dibenzo-p-dioxin at ambient temperature 16

FIGURE 5. Schematic of cavity ringdown spectroscopy (CRDS) apparatus 21

FIGURE 6. Schematic of the laser-induced fluorescence spectrometry technique. 22

FIGURE 7. Schematic of isotopic energy shifts and the associated LIF spectrum. 22

FIGURE 8. Cavity ringdown spectrum of mercury in the air-ICP. . . 23

FIGURE 9. Spectral intensity at different LTSD for Ferro and TVS 28 glasses 28

FIGURE 10. Schematic of the transportable calibration test stand for diagnostic instrumentation 39

FIGURE 11. Scale model of West Valley submerged bed scrubber. . . 41
FIGURE 12. Vapor pressure over aqueous sodium nitrate solutions at 25˚C. 62
FIGURE 13. Comparison of predicted and experimental sulfate concentrations for Tank TX-113 saltcake 66
FIGURE 14. Block diagram of the laboratory-scale salt well pumping apparatus 73
FIGURE 15. Flow stream temperatures with no flow to the heat exchangers. 74
FIGURE 16. Channel fluid temperatures with all four heat exchangers operated at 0.3 gpm 75
FIGURE 17. Pressures measured in the flow loop during pumping of water 76
FIGURE 18. Visual observation of the SX-104 surrogates at 40˚C. . . 78
FIGURE 19. Polarized light microscope image of the ORNL surrogate, 40˚C 100x magnification 78
FIGURE 20. PLM image of Sample 8, 40˚C, 100x magnification . . . 79
FIGURE 21. Prediction of the heat capacity for Sample 8 based on ESP 83
FIGURE 22. Flow loop thermocouple and pressure transducer traces during one of the test runs 85

List of Tables

TABLE 1. Comparison of measured isotopic abundance (in air-ICP) with the theoretical values 23

TABLE 2. Relative precision at different LTSD obtained from a TVS 28 sample 29

TABLE 3. Relative precision at different LTSD obtained from a Ferro glass sample 29

TABLE 4. Temperatures affected by the target surface emissivity in Planck's function assuming apparent blackbody temperature = 1500˚C with 0.9 m as effective wavelength. 56

TABLE 5. Major constituents in saltcakes examined (weight % of sample) 63

TABLE 6. Tank 241-SX-104 supernate surrogate compositions . . . 77

TABLE 7. Solids compositions and phase information for Sample 8 SX-104 surrogate 80

TABLE 8. ESP predictions for Sample 8 at different temperatures. 82

Executive Summary

The Diagnostic Instrumentation and Analysis Laboratory (DIAL) at Mississippi State University (MSU), in accordance with Cooperative Agreement No. DE-FC26-98FT40395, will undertake four tasks for DOE EM during the period April 1, 2000 through March 31, 2001.

Characterization of Heavy Metals, Radionuclides and Organics in Heterogeneous Media

Volatile organic compound monitoring using diode lasers. A significant number of DOE needs are associated with applications requiring small, robust, and sensitive sensors for toxic volatile organic compounds (VOCs). This report describes our progress in developing diode laser cavity ringdown spectroscopy (DL-CRDS) for VOC monitoring. During this quarter, a new DL-CRDS system was constructed and preliminary characterization of system performance (e.g., baseline stability) was initiated. Qualitative data was acquired following the introduction of a small quantity of chlorobenzene into the ringdown cell. Future improvements to obtain quantitative data are described in this report.

Sensitive detection of toxic chlorinated organic compounds. The near ultraviolet absorption spectrum of dibenzo-p-dioxin at ambient temperature has been obtained by cavity ring-down spectroscopy. This is the first cavity ring-down spectrum for a dioxin species and spans about 37 nm. The spectrum shows some structure and is quite congested due to the many internal states populated at ambient temperature. Nevertheless, it shows a characteristic, pronounced peak near 295.8 nm that could be used for diagnostic purposes. Similar work has been initiated on chlorinated dioxin.

Laser-induced breakdown spectroscopy as a process monitor and control for waste thermal treatment. To expand and enhance the laser induced breakdown spectroscopy (LIBS) technique as a process control device for waste processing operations, an investigation to determine methods for improving the calibration of LIBS of solid samples was conducted. The effects of the focal lens to sample surface distance on the LIBS measurements' precision and sensitivity were studied. We found a shorter lens-to-surface distance can improve both LIBS' sensitivity and precision.

Environmental Control Device Testing

Performance enhancement of the ionizing wet scrubber. DIAL currently is in possession of an ionizing wet scrubber (IWS) provided for testing by Ceilcote, Inc. This scrubber is currently a part of the off-gas system at the TSCA-Oak Ridge incineration facility, and is under consideration for use in the DOE waste treatment processes. Current plans are to primarily investigate the relationship of plate voltage with respect to particulate removal in this system. Since the system is a commercial scale system with high flow rates, we had anticipated getting a loss of weight particulate feeder from the one-tenth scale combustion facility at the Savannah River site and installing it at our site. This would give us a particulate feed rate compatible to what is

required for testing. The IWS has been set up at the DIAL facility, and we are in the process of acquiring the particulate feed system.

Testing of a ceramic regenerative heat storage device for dioxin control and heat recovery. A novel regenerative heat recovery device promises to reduce dioxin emissions from incinerators, in addition to recovering waste heat for preheating the combustion air. During this quarter, the detailed design of a prototype was completed, supplies and materials for its construction were ordered, and fabrication began in DIAL's shop facility.

Transportable calibration test stand for diagnostic instrumentation. A transportable calibration test stand is being developed for the purpose of construction of a test train to be used for calibration of optical diagnostic instrumentation. In this quarter, we developed a schematic and engineering drawings for construction of this test stand. We have assembled a pre-heater and two mass flow controllers for air and propane injection into this 2-in. diameter combustion system. The dopant is injected into the stream using a conventional nebulizer, although we will be trying an acoustic injection system. The DIAL LIBS system is currently being used to measure metals concentrations in preheated air on this test bed.

Evaluation and performance enhancement of a submerged bed scrubber. This task is aimed at the evaluation and performance enhancement of a submerged bed scrubber for cleanup of effluent gas from low flow rate incineration systems. We have completed the engineering drawings for the test system and are in the process of acquiring materials to assemble the test bed.

Waste Treatment and D&D Support: Process Monitoring and Control

Dioxin and PCB studies. The formation of dioxins and furans during combustion processes has become a significant focus of concern over the past few years. EPA has initiated an intensive effort to characterize the different sources of dioxins in the United States and to reduce the overall annual rates of emissions. The 1999 MACT for Hazardous Waste Combustors establishes an emission limit for dioxins and furans that will be technically difficult to achieve. Large strides to controlling dioxin and furan emissions from combustion processes will most easily come from an enhanced understanding of their mechanisms of formation. The work being conducted by DIAL will seek to reduce uncertainties associated with the locus of formation of these compounds and factors that contribute to their formation.

Feed stability and chemistry. Details of the design, construction, testing, and evaluation of a laboratory-scale saltwell pumping apparatus are given. The flow loop was developed to aid tank farm operators at Hanford by providing baseline data on supernate transfers from single-shell tanks. Previous efforts at the site have lead to pipeline plugging and associated delays in processing the waste. Work focused on the use of a surrogate for Hanford tank 241-SX-104. Screening experiments were conducted in the laboratory, and ESP calculations were performed. Experiments in the test loop revealed plug formation from trisodium phosphate dodecahydrate. This material has been observed to form long, rod-like crystals and will bind additional water in the solution. If present in significant amounts, the rods form secondary bonds and a three-dimensional structure results. Variations in pressure and temperature were observed during plug formation.

Saltcake dissolution. ESP predictions for sodium nitrate solutions at high ionic strength have been compared to both lattice model predictions and literature data. A method of pre-processing laboratory sam-

ples for low-water content saltcakes has been identified and used to treat data for saltcakes from tanks S-102 and TX-113. ESP has been used to model series dissolution experiments on these saltcakes. The need for a specialized database to provide fundamental thermodynamic data for saltcakes containing a high percentage of sulfate has been identified through examination of preliminary simulation results for TX-113 saltcake. Experimental solubility measurements for the sodium-fluoride-sulfate double salt system are in progress.

Diagnostic Field Applications Coordination and Testing Support (DFACTS)

As part of the DIAL/DOE Cooperative Agreement, a diagnostic field applications, coordination, and testing support (DFACTS) program has been initiated. The DFACTS program addresses the need for on-site measurement of various performance parameters employing DIAL's field applications measurement systems. This aids in the rapid demonstration and implementation of modern fieldable diagnostic methods by providing on-site measurements with DIAL's diagnostic systems and by coordinating and supporting demonstration field tests of instrumentation systems from diagnostic developers within the private sector. Moreover, these on-site measurements provide direct testing support to the DOE complex. This not only provides information for evaluating the applicability of measurement techniques, but also provides a significant add-on-value to the testing efforts being carried out across the DOE complex. This testing support is a major element and advantage of the plan. One major advantage of DIAL involvement is that, because the measurements are made by an independent third party, they also carry more weight in convincing stakeholders that the particular process is effective.

TASK 1

Characterization of Heavy Metals, Radionuclides and Organics in Heterogeneous Media

Volatile Organic Compound Monitoring Using Diode Lasers

C. B. Winstead

Introduction

The United States Department of Energy currently operates three mixed waste thermal treatment facilities (the TSCAI at Oak Ridge, WERF at INEL, and CIF at Savannah River). A concern for these and future DOE facilities is monitoring and controlling the release of volatile organic compounds in the facility off-gas. For example, at least five needs are listed in the year *2000 DOE Needs Database* that directly request continuous emission monitors (CEMs) for species including organics. Of these five listed needs, four (SR00-1004, ID-2.1.18, ID-S.1.02, and ID-2.1.41) are rated as Priority 1 needs, implying that they are critical to the success of a given mission. The fifth (ID-3.2.32) is rated as Priority 2, indicating that a substantial benefit would be realized if the need were fulfilled. According to the *Savannah River Site Need Statement* (full text available at http://www.srs.gov/general/srtech/stcg/Needs/sr-1004.htm), for CEM purposes the desired detection limit for most organics other than dioxins is approximately 1 ug/m^3. This corresponds in general to detection

limits in air just below the parts-per-billion range (e.g., 1 ug/m^3 of chlorobenzene or trichloroethane is approximately 0.2 ppb). In addition, solutions for numerous other organic monitoring applications are needed throughout the DOE complex (e.g., organic species in groundwater).

This project is a continuation of our previous work that focused on the evaluation of near-infrared diode laser spectroscopy for monitoring selected volatile organic compounds (VOCs) in air. That work utilized simple multipass absorption techniques to determine the effect of pressure broadening on the sensitivity of VOC detection at available diode laser wavelengths. Extrapolating from these experimental results for VOCs in air suggests that a technique known as diode laser cavity ringdown spectroscopy (DL-CRDS) could potentially achieve CEM level detection limits with no preconcentration. While our previous multipass absorption experiments indicated a detection limit of 20 ppm for benzene, DL-CRDS should be four to six orders of magnitude more sensitive. This level of detection is approximately equal to just slightly worse than the sensitivity required for an organic CEM. Therefore, an experimental evaluation of the achievable detection limits for VOCs using DL-CRDS is needed. The primary objective of this project is to construct a laboratory DL-CRDS system and determine its detection limits for selected VOCs. This information will be used to determine if a DL-CRDS system should be constructed for process gas monitoring next year.

The data gathered this year will also be used to guide the design and construction of an appropriate sampling interface for VOC measurements. Although it may be possible that a very advanced DL-CRDS system could achieve CEM detection limits directly in an off-gas sample (pending the effects of pressure), for a robust industrial system it may be preferable to use preconcentration in a sampling system to reach lower detection limits. Preconcentration using adsorbent or cryotrap technology (e.g., a “purge and trap” method) is well developed for on-line gas chromatography (GC). The potential sensi-

tivity of a DL-CRDS system should allow minimal preconcentration (10X - 50X) to be used, allowing for rapid measurements (e.g., every 15 minutes) without the operational complexity, maintenance, and calibration issues associated with GC. Thus, this year's laboratory measurements are essential to guide the design for the next year's sampling system. This work will also clarify our capabilities for meeting other DOE needs such as monitoring underground organic plumes, making perimeter or ambient air VOC measurements, or potentially monitoring particulate concentrations at very low levels.

Work Accomplished

An infrared diode ringdown system was assembled and ringdown waveforms were captured. Figure 1 depicts a ringdown signal obtained using an infrared wavelength distributed feedback diode laser. This waveform was acquired using a "frequency shift" method that allows for fewer optical components in the system hardware

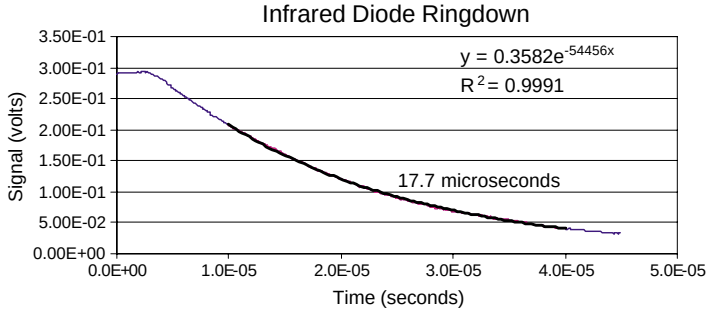

FIGURE 1. Ringdown signal obtained using an infrared-wavelength distributed feedback diode laser.

without sacrificing stability. This method is applicable to broad line-width spectra like those of the VOCs we will be measuring. An excellent stability corresponding to a 0.26% variation of the signal baseline was achieved with the infrared ringdown system, although achieving such stability still requires considerable adjustment at the moment.

Note that with standard pulsed laser ringdown, 1% baseline standard deviation is considered the norm.

Chlorobenzene was introduced into the ringdown cell for an initial qualitative test of the operation of the infrared system. The gas phase chlorobenzene was introduced into the system from a small vial containing liquid chlorobenzene. The residual air in the vial was evacuated while the chlorobenzene was frozen in liquid nitrogen, yielding pure chlorobenzene vapor in the headspace of the vial after the chlorobenzene thawed. Figure 2 depicts the response of the infrared ringdown system when a small amount of chlorobenzene is introduced into the cell. The quantity of chlorobenzene introduced was too small for our gauges to accurately measure, so this plot represents only qualitative data. The step-like structure visible as the signal rises back to the baseline results from opening the vacuum valve briefly to pump out a small fraction of the chlorobenzene in the cell. The baseline is reached again when all the chlorobenzene is pumped out. Although this is only qualitative data, it does demonstrate that the system is thus far performing as expected. A new gas handling system will allow us to quantify these results.

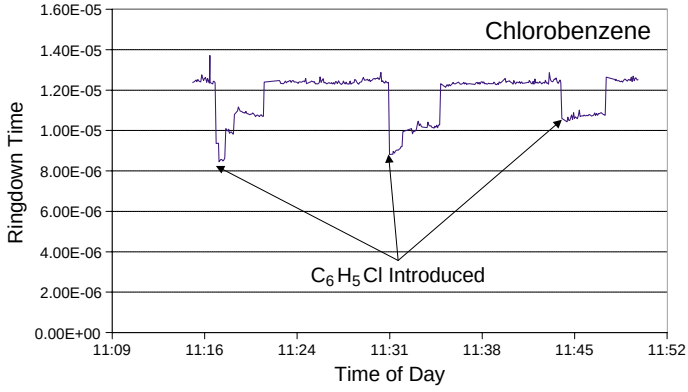

FIGURE 2. Response of the infrared ringdown system when a small amount of chlorobenzene is introduced into the cell.

Work Planned

During the next quarter, we will work to improve our baseline stability even further. This will be accomplished at least in part by mechanical changes to the cell that will be required to allow us to cycle from vacuum to atmospheric pressure conditions without significant alteration of the cavity alignment. In addition, a new gas handling system will be constructed to allow the expansion of a high concentration of gas in a small volume into the larger volume of the measurement cell. The volume ratio of the two cells will be used to calculate the concentration of analyte in the measurement cell to allow quantitative data acquisition with a known concentration of analyte.

Nomenclature

TSCAI	Toxic Substances Control Act Incinerator
WERF	Western Experimental Reduction Facility
CIF	Consolidated Incineration Facility
VOC	volatile organic compound
CEM	continuous emission monitor
GC	gas chromatography
DL-CRDS	diode laser cavity ringdown spectroscopy

Metal Continuous Emission Monitors (APO-GEM)

George Miller

Introduction

Air plasma off-gas emission monitor (APO-GEM). Over the last twenty years, the use of argon ICP-AES for the measurement of trace elements in solution has matured into a standard analytical technique. However, unlike the laboratory ICP, it is essential for a CEM that the system be hardened sufficiently to handle the problems of a real world environment. These problems include the ability to readily tolerate the introduction of a variety of molecular gas matrices, significant variations in moisture and particle loading, as well as the thermal, vibrational and clogging problems found outside the laboratory. The system under development at DIAL has taken the advantages inherent in inductively-coupled plasma technology and incorporated them into an APO-GEM, a CEM capable of tolerating the real world environment while accurately measuring the real time concentration of metals in exhaust stacks.

Elemental mercury monitor. Of special interest to both DOE and EPA is that of mercury measurement. Mercury is one of the materials on the list of heavy metals that will be regulated by the proposed EPA rule for waste incinerators. It is also a problem for tank waste processing, decontamination and decommissioning, and hot cell operations throughout DOE. The emission-based CEM techniques being developed and tested by DOE and the EPA are less sensitive to mercury vapor than techniques based on atomic absorption. Many of these emission techniques, although not ICP-AES, are limited in accuracy and sensitivity to mercury vapor by self-absorption by cold atomic mercury vapors, particularly for in situ techniques. APO-GEM yields a measurement of the total mercury present in an exhaust stream. Therefore, an absorption-based technique is preferable to

emission techniques for monitoring elemental mercury vapor. Significant improvements in sensitivity and accuracy of the detection of mercury by cold vapor atomic absorption (CVAA) may be realized by using a high-resolution spectrometer for detection of transmitted light. The successful development of this instrument in combination with APO-GEM would provide a real time method for directly determining both the total and elemental mercury concentrations.

Work Accomplished

During this period, cavity ringdown spectroscopy was employed to evaluate the viability of coupling it with the air plasma off-gas emission monitor (APO-GEM) to enhance the detection of elemental mercury present in exhaust gases. That is, cavity ringdown data was obtained using an air inductively coupled plasma system as an atomization source.

The high rf power necessary to maintain an atmospheric air plasma did impact the performance of the system as compared to a low power argon inductively coupled plasma (ICP). However, the potential of the cavity ringdown technique can be seen in the preliminary isotopically resolved spectra for Hg obtained in the air plasma systems. These results are outlined in the section titled *Isotopically Selective Monitors for Transuranic Elements* of the chapter.

Mercury Monitor

Information regarding the mercury species present in exhaust gas is important for both pollution and combustion control. While atomic mercury in exhaust gas can be determined directly by atomic absorption spectrometry (AAS), for molecular mercury species (such as $HgCl_2$) it is necessary to convert the molecular species to atomic mercury for AAS measurement. Several methods are used to do this. One method is pyrolysis. In this case, a quartz tube is heated to a temperature higher than 500°C to dissociate the mercury species. An alterna-

tive way to convert molecular mercury to mercury atom is by using chemical reduction. In fact, cold vapor generation coupling with AAS is the most widely used method for the determination of mercury in aqueous solution. In this method, mercury (II) compounds in solution are reduced by reduction reagent ($SnCl_2$ or $NaBH_4$) and then the produced mercury is purged out of the solution by using a carrier gas. However, there are problems with this method, including reduced sensitivity of the method by the dilution this purging brings. Secondly, it introduces water droplets into the absorption cell which interfere with the AAS measurement. Moreover, the cold vapor AAS (CV/AAS) method is a batch method. Mercury atoms, however, are already produced in aqueous solution during cold vapor generation process. Therefore it would not be necessary to separate mercury atoms from aqueous solution if we can measure mercury AAS signal in aqueous solution. Based on this approach, an on-line real time mercury monitoring system could be developed. As our collaborators at Ames Laboratory are studying the pyrolysis method, we decided to evaluate this approach.

Preliminary experiments to measure elemental mercury in aqueous solution were carried out by using a simple flow cell. Mercury standard solution and $SnCl_2$ solution were pumped and merged before entering the flow cell and the mercury AAS signal was recorded. Based on these results, we reached the following conclusions:

- Mercury can be observed in aqueous solution using AAS.
- A redesigned flow cell would increase sensitivity. At present, the absorption pathlength is approximately 2 mm. A flow cell with much longer pathlength would increase the sensitivity and improve the stability of the signal.
- Interferences: by using $SnCl_2$ as the reduction reagent, only noble metal ions such as Cu^{2+}, Ag^{+}, Au (III), Pt vent line (IV), Pd^{2+} would introduce interferences. However, these elements are usually not in waste solutions.

- On-line real time monitoring of mercury in solution can be realized.
- The instrument is simple and easy to operate.

Sensitive Detection of Toxic Chlorinated Organic Compounds

Ram Vasudev

Introduction

This project addresses the widespread need for a general purpose, sensitive detector for toxic compounds, especially chlorinated organic compounds. Chemicals such as dioxins are generated as unwanted by-products of incomplete combustion and are among the most toxic manmade chemicals. The need for their detection either directly, or through the detection of surrogates/precursors, has been a subject of intense research in many laboratories, including SRI (Menlo Park), DLR (Stuttgart) and EPA (Durham). Popular laser-based methods such as laser-induced fluorescence (LIF) and resonance-enhanced multiphoton ionization (REMPI), although quite sensitive in general, are susceptible to loss in sensitivity due to intersystem crossing (ISC) induced by the presence of chlorine. In addition, the loss in detection sensitivity is a monotonic function of the chlorine content, so for polychlorinated molecules the detection limits can be compromised. To circumvent this spectroscopic problem, we have been exploring a relatively new technique called cavity ring-down spectroscopy (CRDS). It is solely absorption-based and is thus not influenced by excited-state nonradiative decay, as shown by our work on chlorinated benzenes with varying chlorine content.[1-2] It is quite sensitive and, in principle, simple to implement, so it is a very promising universal toxic gas detector. This report describes our ini-

tial work towards developing a CRDS-based detector for dioxin-type molecules.

Experimental Technique (Cavity Ring-down Spectroscopy)

As mentioned in our earlier reports, the high sensitivity of CRDS is due to the very long absorption pathlengths achieved by trapping a laser pulse between the mirrors of a high-finesses (low loss) optical cavity. In suitable cases, the optical absorption pathlength can be several kilometers even though the cavity itself is considerably shorter ($\leq$ 1 m), so very small concentrations of chemical species can be detected. Our CRDS setup is shown schematically in Figure 3.

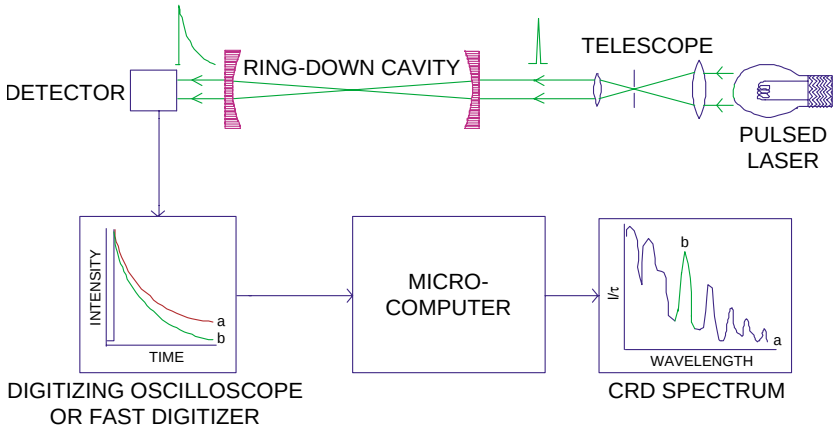

FIGURE 3. Schematic diagram of the CRDS setup.

In the present work, the laser used is a tunable dye laser operating in the 530 - 610 nm region. The dye laser output is frequency-doubled and injected into the CRDS cell containing the sample, and the cavity transmission is monitored by a photomultiplier. The “ring-down” decay signal is captured by a fast transient digitizer and stored on a computer. The data is processed by simple programs to generate absorption spectra.

Work Accomplished

Dioxin Monitor

As a first step towards developing a detector for dioxins, we have recorded the spectrum of dibenzo-*p*-dioxin by CRDS. Our initial findings are summarized in Figure 4, which shows the near ultraviolet spectrum recorded at ambient temperature (300 K). The spectrum is quite extensive, as expected for such a large molecule. The spectrum in the 265 - 301 nm range is thought to be composed of two singlet←singlet electronic transitions with the origin bands located near 295.9 and 291.5 nm. The spectrum shows some structure and is quite congested because many internal states are populated at ambient temperature. This includes (a) several thousand rotational states and (b) low-frequency vibrational states such as those involving the butterfly vibration of the phenyl rings about the two oxygens. Be that as it may, the spectrum shows a characteristic, pronounced peak near 295.8 nm, which could be used for diagnostics at ambient temperature.

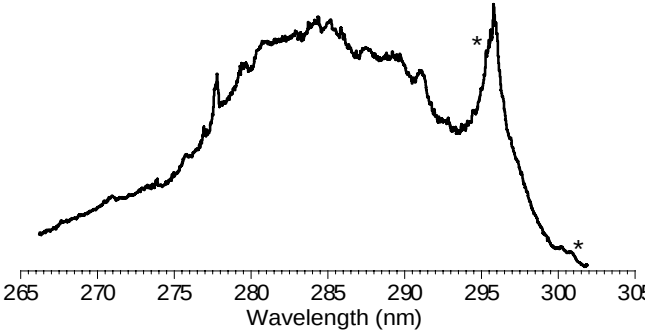

FIGURE 4. Cavity ring-down spectrum of dibenzo-*p*-dioxin at ambient temperature. Note that the small oscillations, shoulders and bumps such as the ones identified with asterisks are genuine, reproducible spectroscopic features an.

Dioxin Precursors/Surrogates

Work is continuing on this class of molecules. The emphasis is on detection limits and species specificity. Our current lowest detection limit is in the ppb range.

Data Acquisition Software

Concurrent with the experimental work, we are developing real-time data acquisition software.

Future Work

Work will continue our work on dioxins and dioxin surrogates/ precursors.

References

1. *Instrumentation Development, Measurement and Performance Evaluation of Environmental Technologies,* Quarterly Technical Progress Report for US DOE Cooperative Agreement No. DE-FC26-98FT40395. DIAL 40395-7, p. 26.

2. I. Tretiakov and R. Vasudev, under preparation (to be published).

Isotopically Selective Monitors for Transuranic Elements

D. L. Monts and C. B. Winstead

Introduction

A number of DOE needs have been established that are related to the treatment or characterization of waste contaminated with uranium

or transuranic (TRU) elements. For example, the Hanford site lists as needs the development of a technology for treating TRU waste contaminated with PCBs and ignitables (Need RL-MW06) and the development of a sensitive screening method for selected transuranic elements in soils in a near real time manner (Need RL-SS-14). Although these needs are very different in nature, each will no doubt require the development of a robust, yet sensitive detection system capable of quantifying TRU element concentrations with isotopic resolution. Such a system would serve as a process monitor in one case and as an on-site analytical tool in another. In addition to needs listed in the DOE needs database, the Idaho National Engineering and Environmental Laboratory (INEEL) has expressed a need for monitoring residual TRU elements in treated high level waste. Specifically, a need exists for on-line monitoring of the low activity fraction of this treated waste after dissolution and partitioning. Such a system could replace expensive off-line sampling and analysis and eliminate the need for holding tanks in the Idaho HLW process. This project is primarily directed toward on-line monitoring application and thus is most relevant to the efforts of the High Level Waste Tank Remediation Focus Area. However, future applications of the developed technology should make this effort relevant to additional needs in process control and on-site monitoring.

In spite of their radioactivity, detecting TRU elements at ultrasensitive levels has proven to be problematic for traditional radiological counting methods due to the very long half-lives of these predominantly alpha-emitting elements. A new approach is required to allow for rapid measurement of TRU elemental concentrations in an on-line or rapid on-site manner. Optical spectroscopic methods offer significant promise in such an application and are capable of reaching detection limits far below counting techniques in a very short measurement period.

This work is concerned with the evaluation of two sensitive laser spectroscopic methods, laser-induced fluorescence (LIF) and cavity

ringdown spectroscopy (CRDS), for potential use as TRU monitors. In laser-induced fluorescence, a laser is used to excite atoms of the selected element from one electronic state to another. The subsequent fluorescence emitted by the excited atom is monitored using a spectrometer and photomultiplier tube arrangement. Under appropriate conditions, the fluorescence intensity is directly proportional to the concentration of the element. In cavity ringdown spectroscopy, the time for a laser pulse to decay in an optical cavity is measured. Analyte atoms introduced into the cavity reduce this “ringdown” time by absorbing light from the laser pulse. For both the LIF and CRDS efforts, atomic species will be generated by injecting standard or surrogate sample solutions into an inductively coupled plasma (ICP). The first step of both the LIF and CRDS processes is the same, namely absorption of laser photons by analyte atoms. The isotopic resolution of each technique is achieved in this first step by using a narrow linewidth laser to excite only one particular isotope of the element being measured. Although CRDS theoretically will detect all absorption events and thus might be expected to be the more sensitive of the two techniques, the simpler implementation and better signal-to-noise ratio of LIF could result in LIF being the preferred monitoring technique. Experimental evaluation of each technique is required. Recent regulatory approval for the use of uranium in our facility will allow this evaluation to proceed.

Purpose

The primary purpose of this project is to evaluate LIF and CRDS for use as robust, isotopically selective, cost-effective, on-line TRU monitors for the INEEL high level waste processing facility. Knowledge of isotopic abundances is necessary since different isotopes can have widely differing activities. The niche for this technique is determination of concentrations and isotopic abundances for cases where current techniques are severely limited by low throughput, such as (1) cases where the radioactivity is so low that radioactive decay disintegration counting techniques cannot analyze samples during accept-

able counting periods; and (2) cases where lengthy sample preparation is required for mass spectrometric determination. The performance of these techniques will be evaluated using uranium standards and surrogate waste solutions provided by INEEL. The successful development and implementation of a TRU monitor could save millions of dollars through the elimination of holding tanks currently planned for the INEEL process. These tanks would be used to hold the treated waste prior to release while TRU analyses are performed on the tank contents. Clearly, this particular effort is most relevant to the effort of the High Level Waste Tank Remediation Focus Area. However, such a system could ultimately provide solutions for needs in other focus areas such as Mixed-Waste Characterization, Treatment, and Disposal. At the end of this project, a full analysis of the sensitivity and selectivity of LIF and CRDS for uranium monitoring will be reported, and recommendations for how to proceed in the construction of an isotopically selective, on-line TRU monitor will be presented.

Methodology

Cavity ringdown spectroscopy. Cavity ringdown spectroscopy (CRDS) is an extremely sensitive variant of absorption spectroscopy that has been demonstrated in a variety of studies. Thus the ringdown technique will be only briefly summarized here. In the original form of CRDS, a laser pulse from a tunable pulsed laser is introduced into a stable optical cavity formed from two highly reflective mirrors (Fig. 5). A fraction of the laser pulse is injected through one cavity mirror and is trapped, propagating back and forth between the mirrors. A photomultiplier tube placed behind the second cavity mirror is used to monitor the time constant for the pulse to decay (also known as the “ringdown” time). The reflectivity of the mirrors and the absorption of a sample in the cavity determine the pulse decay time. The pulse interacts with an absorbing medium in the cavity over the course of potentially thousands of round trips, vastly increasing CRDS sensitivity over standard absorption methods. As the absorption in the cavity

increases, the increased optical losses cause the decay time for the light in the cavity to decrease. By inserting into the cavity an appropriate atomization source, such as an inductively coupled plasma (ICP), very low concentrations of the various chemical forms of TRU elements can be atomized and detected by measuring changes in the cavity ringdown time constant.

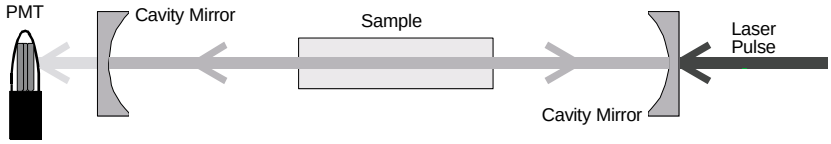

FIGURE 5. Schematic of cavity ringdown spectroscopy (CRDS) apparatus.

Laser-induced fluorescence spectrometry. Laser-induced fluorescence (LIF) spectrometry is a well-established, robust technique for detecting species of interest at low concentrations. In the LIF technique (Fig. 6), an electronic state of the species of interest is excited with a tunable laser and the resulting fluorescence intensity is monitored as a function of laser wavelength. Since the mass of isotopes are different from one another, the corresponding atomic energy levels are slightly different (Fig. 7). Consequently, when a sufficiently high-resolution, tunable laser is scanned across an atomic electronic transition, the resulting LIF spectrum contains a peak associated with each isotope present; the intensities of the isotopic peaks are directly related to the concentration of the isotope. Hence, the isotopic abundances can readily be obtained from the LIF spectrum. In order that the individual isotopic transitions can be resolved, it is necessary that the species of interest be in the gas-phase. For the TRU elements of interest, an atomization source is required in order to volatilize and atomize the sample. A calibration curve is obtained by recording the LIF signal intensity as a function of concentration. Using the calibration curve, unknown concentrations can be determined.

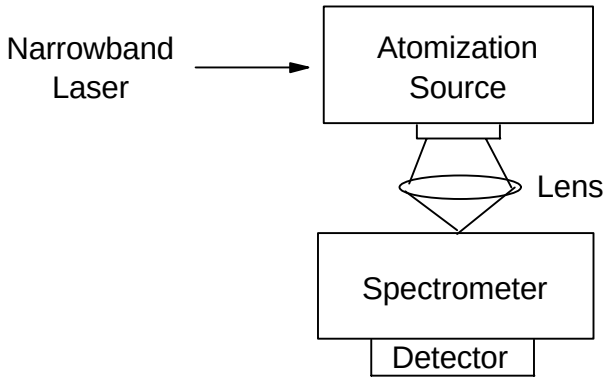

FIGURE 6. Schematic of the laser-induced fluorescence spectrometry technique.

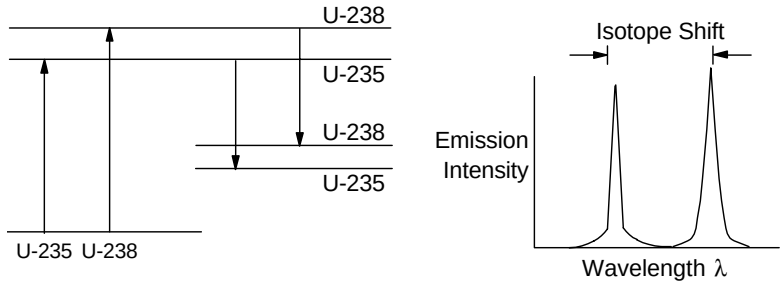

FIGURE 7. Schematic of isotopic energy shifts and the associated LIF spectrum.

Work Accomplished

Cavity Ringdown Spectroscopy

During the time period from April - June, 2000, cavity ringdown efforts centered on completion of data acquisition for mercury in an inductively coupled plasma. Two significant components of this work are directly related to development of an isotopically selective monitoring system for radionuclides. First, cavity ringdown data was obtained using an air inductively coupled plasma system as an atomi-

zation source. A comparison of air and argon plasma performance will be needed for a final decision on a monitor system. Secondly, preliminary isotopically resolved spectra for Hg were obtained in both the air and argon plasma systems. In both cases, as demonstrated in Table 1, the measured isotopic abundances were in excellent agreement with established values. The isotopic results for the air ICP system are displayed in Figure 8. For mercury, where a neutral atomic transition is monitored, the argon plasma detection limits were far below the corresponding air limits. However, for uranium, where ionic species will likely be monitored, the relative performance of the air plasma may improve.

TABLE 1. Comparison of measured isotopic abundance (in air-ICP) with the theoretical values.

Line #	Wavelength (nm)	Experimental Ratio (%)	Theoretical Ratio (%)	Isotope Assignments
1	253.6466			201 + 199
2	253.6498	13.9	16.6	198 + 201
3	253.6517	28.5	26.7	200
4	253.6528	34.9	34.5	202
5	253.6535	22.7	22.1	204 + 201 + 199

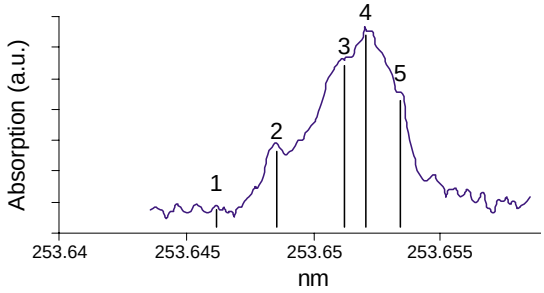

FIGURE 8. Cavity ringdown spectrum of mercury in the air-ICP. A 3-point smooth is applied to the data before plotting. The vertical lines indicate the positions of the various mercury isotopic signatures.

Laser-induced Fluorescence Spectrometry

Our efforts to optimize operating conditions using Eu (a uranium surrogate) in an ICP plasma continued. During the last reporting period, construction of the dedicated vent line with HEPA filter was completed. During the current reporting period, both LIF and CRDS discovered that the dedicated vent line exhaust provides too great a draft, causing the ICP plasma to swirl. Perturbation of the ICP plasma by the exhaust hinders optimization because it is difficult to distinguish between fluctuations due to exhaust-induced turbulence and signal changes due to changes in operating conditions. Therefore, the dedicated vent line was modified in the LIF laboratory to reduce the draft. Preliminary visual tests indicate that the ICP plasma fluctuations with and without the vent line exhausting are now about the same. Preliminary LIF experiments using two different Eu solutions at one ICP rf power and under one set of flow conditions indicate that there is no significant perturbation of the LIF signal by vent line exhaust. We plan to perform more LIF experiments (employing different ICP rf powers, different solution concentrations, and different surrogates) to verify that the vent line exhaust is not affecting our results before beginning experiments with radioactive materials.

During this reporting period, our progress was slowed by equipment failure of two components of the LIF system. The equipment was repaired to enable experiments to continue and replacements have been ordered.

Work Planned

Cavity Ringdown Spectroscopy

All personnel associated with this project are scheduled to have completed the university required radioactivity safety course within the next two weeks. Following minor laser repairs, the next major emphasis will be to optimize the CRDS laser system for narrow line-

width operation at a uranium absorption wavelength. It is anticipated that during the next quarter, we will obtain uranium ion spectra in an argon ICP and begin efforts to optimize plasma and detection parameters for optimum detection sensitivity.

Laser-induced Fluorescence Spectrometry

We have begun a series of experiments using argon as the carrier gas and surrogates, such as Eu, to verify that the exhaust draft is not significantly perturbing the LIF results and then to continue optimization of the ICP system. Once initial optimization is completed, we will begin work during the next quarter on uranium as the analyte species. At that point, our efforts will concentrate on optimization of operating conditions for detection of uranium in an ICP plasma. Parameters to be optimized include carrier gas flow rate, position of the laser excitation beam within the plasma, choice of excitation and detection transitions. Since the CRDS group is also utilizing an ICP plasma source for their efforts and hence also needs to optimize their ICP plasma for uranium detection, the two groups will split the effort and share results; this will enable us to more extensively survey parameter space and to more quickly arrive at the optimum operating conditions.

A prerequisite for successful completion of this project is a sufficiently narrow linewidth, tunable laser system that can be reproducibly scanned. After optimization using naturally occurring uranium and our current dye laser, we, in collaboration with the CRDS group, will perform experiments using CRDS' moderately high-resolution dye laser system to evaluate whether or not that laser is sufficiently narrow to isotopically resolve uranium. If, as expected, these LIF experiments prove that such a moderately high resolution tunable laser system has sufficient resolution for uranium, then a comparable dye laser system will be purchased for this effort; if those experiments indicate that even higher resolution is required, then additional

funding will be sought in order to purchase an ultra high resolution tunable laser system.

Nomenclature

CRDS	cavity ringdown spectroscopy
DIAL	Diagnostic Instrumentation and Analysis Laboratory
DOE	U. S. Department of Energy
HLW	high level waste
ICP	inductively coupled plasma
INEEL	Idaho National Engineering and Environmental Laboratory
LIF	laser-induced fluorescence
PCB	polychlorinated biphenyl
rf	radio frequency
TRU	transuranic

Laser-induced Breakdown Spectroscopy

C.F. Su, F.Y. Yueh and J.P. Singh

Introduction

This technical task has been focused on the development and application of laser-induced breakdown spectroscopy (LIBS) to monitor RCRA metals from thermal treatment processing facilities. LIBS is a laser-based, non-intrusive, and sensitive optical diagnostic technique for measuring the concentration of various atomic and molecular species in test media.[3,4] It uses a high power laser beam to produce

a laser-induced plasma at the test point. The plasma atomizes and electronically excites the various atomic species present in the test volume in a single step. The intensities of the atomic emission lines observed in the LIBS spectrum are used to infer the concentration of the atomic species. LIBS has successfully demonstrated its real-time monitoring capability in various field tests.[5-10]

Work Performed

In the last several years, the DIAL LIBS group has successfully used the LIBS technique to evaluate the elemental concentration ratios in glass samples. Many experimental parameters such as the laser power, gate delay time, gate width, and optical slit width have been investigated to obtain the optimal condition for the best LIBS spectral measurements. However, due to the laser power variations during the data collecting process, spectral intensity fluctuation was found to be a serious problem on the spectral intensity measurements. In order to minimize the spectral intensity variations, insight into the effect of lens to surface distance (LTSD) was undertaken.

Two glass samples were used for the experiment. They were TVS 28 glass and one powder sample from Ferro Company in Ohio. Before the experiment, both samples were individually held by a crucible and heated to molten state, then cooled to solid state at room temperature. The LIBS spectral intensities recorded at three LTSDs were studied for these two samples. During the experiments, the focus points were set to 7 mm above the sample surface, just on the sample surface, and 7 mm below the surface, respectively. An UV-grade lens of a 30-cm focal length was used to produce the laser-induced spark. Fifty spectra of each experimental setup were collected in 250 seconds.

The wavelength region centered at 360 nm was investigated for the TVS 28 glass. The Ferro glass sample was investigated near 375 nm. The data were recorded when the samples were slowly translated

and also at a fixed position. The spectral intensities of three elements were studied for the TVS 28 glass. Two spectral lines, one strong and one weak, of each element were selected for analysis. They were (in nm): Cr (359.35, 360.53), Fe (358.12, 356.54), and Ti (365.35, 363.55). For the other sample, three elements were also studied. Only one line for each element was used in this analysis. Those lines are (in nm): Fe (371.99), Mg (383.23), and Ti (375.29).

The average spectral intensity and standard deviation of the fifty spectra for each condition were calculated. The relative precision for the data collected from the steady sample was between 45 and 140 percent of the averaged intensity. Those collected from the sample slowly translated, on the other hand, had a lower relative precision (12 - 40%). The standard deviations obtained from the strong and weak lines were found to be in good agreement. Data recorded at the LTSD show that the spectral intensity was stronger when the LTSD was shorter than the focal length. Figure 9 shows the spectral intensity of these two glass samples at different LTSDs. The data were recorded while the sample was slowly translated. Tables 2 and 3 show the relative precision obtained from the three LTSDs for the two glass samples. It is clearly shown that the relative precision also improved when the LTSD was shorter than the focal length.

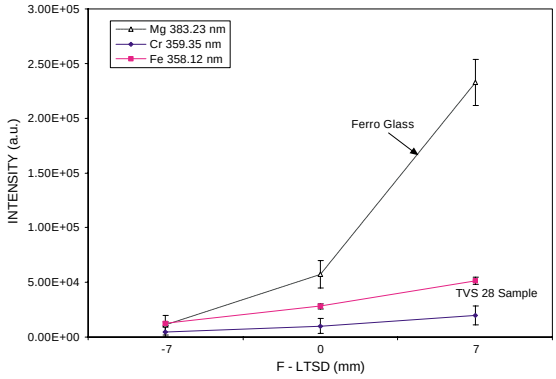

FIGURE 9. Spectral intensity at different LTSD for Ferro and TVS 28 glasses.

The LTSD is a critical parameter for the LIBS measurement of solid and liquid samples. A change of the LTSD of a few millimeters can affect the absolute analyte intensity. This preliminary study shows that precision and sensitivity can be improved by shortening the LTSD. More experiments will be conducted to find the optimum LTSDs for glass measurements. The calibration data will then be collected using the optimum LTSD.

TABLE 2. Relative precision at different LTSD obtained from a TVS 28 sample.

	Relative Precision (%)		
	F-LTSD (mm)		
Spectral Line	-7	0	7
Cr 359.35 nm	38	24	16
Cr 360.53 nm	37	25	16
Fe 358.12 nm	38	25	17
Fe 356.54 nm	39	26	17
Ti 365.35 nm	41	25	13
Ti 353.55 nm	42	25	13

TABLE 3. Relative precision at different LTSD obtained from a Ferro glass sample.

	Relative Precision (%)		
	F- LTSD (mm)		
Spectral Line	7	0	7
Fe (371.99 nm)	65	23	2
Mg (383.23 nm)	80	22	9
Ti (375.29 nm)	72	31	34

Work Planned

Testing of the LTSD for the solid sample will continue to determine an optimum LTSD for LIBS calibration of the solid sample. Preparation for the LIBS CEM measurements in the DIAL test stand will begin.

References

3. D.A. Cremers and L.J. Radziemski. 1987. Laser plasmas for chemical analysis. *Laser Spectroscopy and its Application*, L.J. Radziemski, R.W. Solarz, J.A. Paisner, eds. New York: Marcel Dekker. Ch. 5, p.351.

4. L.J. Radziemski and D.A. Cremers. 1989. Spectrochemical analysis using plasma excitation. *Laser-induced Plasmas and Applications*, L.J. Radziemski and D.A. Cremers, eds. New York: Marcel Dekker. Ch. 7, p. 295-326.

5. J.P. Singh, F.Y. Yueh, H. Zhang. 1997. *Process Control and Qua*lity, 10:247.

6. J.P. Singh, H. Zhang, F.Y. Yueh and K.P. Carney. 1996. *Applied Spectroscopy*, 50:764.

7. J.P. Singh, H. Zhang and F.Y. Yueh. February 1996. Transportable Vitrification System Shakedown Test, Westinghouse Savannah River Corporation and Diagnostic Instrumentation and Analysis Laboratory: Laser-induced Breakdown Spectroscopy Measurements. US DOE Contract No. DE-FG02-93CH-10575. DIAL 10575 Trip Report 96-1.3.

8. J.P. Singh, H. Zhang and F.Y. Yueh. April 1996. DOE and EPA Continuous Emission Monitoring Test at EPA National Risk Management Research Laboratory (NRMRL). US DOE Contract No. DE-FG02-93CH-10575. DIAL 10575 Trip Report 96-2.

9. J.P. Singh, H. Zhang and F.Y. Yueh. 1996. Plasma Arc Centrifugal Treatment PACT-6 Slip Stream Test Bed (SSTB) 100-hour Duration Controlled Emission Demonstration (CED) Test. DIAL Trip Report 96-3.

10. J.P. Singh, H. Zhang and F.Y. Yueh. September 1997. DOE and EPA Continuous Emission Monitoring Test at EPA National Risk Management Research Laboratory (NRMRL). DIAL Trip Report 97-1.

TASK 2

Environmental Control Device Testing

Performance Enhancement of the Ionizing Wet Scrubber

R. ArunKumar

Introduction

The ionizing wet scrubber (IWS) is one of the few effective commercial micron and submicron particulate removal systems used to treat effluent gas from incineration and waste processing systems. The system operates essentially like a wet electrostatic precipitator, but some its theory of operation differs primarily with respect to the development of particulate charges. In this study we plan to enhance the performance of the IWS and overcome some of the problems associated with its operation. Current problems include plate life and performance with respect to plate spacing and applied voltage. Information obtained from this work should enable DOE to operate this particulate cleaning device more confidently.

Base line measurements of the IWS unit will initially be conducted in regards to its performance and particulate removal efficiency. In order to complete this task we will need a particulate feeder of a sufficiently large size to simulate particulate loading at the incinerator facilities. We hope to obtain the feeder that is currently at the

one-tenth scale combustion facility at the Savannah River Site and install it at our site. We will survey the DOE incinerator sites and determine the order of importance of the operational issues that need to be addressed with the IWS. These may include some problems that we have not yet identified. We will then select the most important tasks that we think can be solved in the given time frame. As part of our technology transfer mission, and in exchange for lending the IWS unit to DIAL we will share the information gained with ITEQ, the manufacturers of the unit.

Work Accomplished

The IWS that has been installed at our site has been tested without any particulate feed. The project is currently awaiting the acquisition, delivery and installation of the particulate feeder from the Savannah River Site. The acquisition of the feeder is a specific go/no-go item under this task.

Work Planned

The primary task in the coming quarter will entail acquiring the particulate feeder. Current plans include sending a team of DIAL technicians who will have to undergo training at the site before they can be allowed to dismantle any part of the particulate feeder. Once we take delivery of the system we will be able to install it on the IWS and commence testing.

Testing of a Ceramic Regenerative Heat Storage Device for Dioxin Control and Heat Recovery

O.P. Norton

Introduction

The new MACT standards for dioxins (0.2 ng/dscm TEQ) will challenge incinerator operators, the DOE included. DOE waste remediation facilities that will be impacted by these rules include the Consolidated Incineration Facility (CIF) at Savannah River and the TSCA incinerator at Oak Ridge. Also, we note that the processes that form dioxins and furans could also occur in other thermal waste treatment systems, such as vitrification systems and plasma torch-based systems, so the impact on DOE's EM program could be considerable.

Although our knowledge of dioxin formation mechanisms and kinetics is incomplete, it is generally accepted that dioxins and furans are formed as combustion products (flue gases with associated particulates and products of incomplete combustion) and cooled downstream of the combustor. Tuppurainen, et al.,[11] give the dioxin formation range as 250 to 650ºC, with the maximum at about 300ºC. Karasek and Dickson[12] found that the optimum temperature range for the formation of dioxins from pentachlorophenol was 250 to 350ºC. Altwicker, et al.,[13] give the critical temperature range as 250 to 400ºC. Although these different sources report slightly different critical temperature ranges for dioxin formation, it is fairly clear that dioxins and furans are formed at fairly low temperatures, as the combustion products cool.

This insight suggests that dioxin could be controlled by quenching--cooling the exhaust gases as quickly as possible through this critical temperature band. Rapid quenching is indeed a common

dioxin control mechanism in municipal solid waste incinerators, and dioxin formation can be minimized by this strategy.[11]

Santoleri and Budin[14] report: “Systems that are able to quench the high temperature combustion gases from 1000 - 1200ºC to adiabatic (75 - 90ºC) in fractions of a second have emissions well below the levels established by the MACT standards (0.2 ng/dscm TEQ).”

Thus, rapid quenching--cooling the flue gases through the critical temperature range as quickly as possible--is an effective method of dioxin control. Water sprays have been effective for dioxin control, but this method essentially wastes the thermal energy in the combustion products. Also, for hazardous and radioactive waste incineration, a secondary waste stream will be created.

We propose that a regenerative heat recovery system can be used to control dioxin emissions. Regenerators have long been used to recover waste heat from flue gases, using this heat to preheat the incoming combustion air. We observe that, if the cooling of the hot gases in the regenerator is sufficiently rapid, then dioxin formation should be minimized as well.

A novel regenerative heat storage device is proposed that can be used to suppress dioxin formation in the off-gas of a thermal waste treatment plant. The flue gas is rapidly cooled as it passes through the device to prevent the formation of dioxins and furans from the precursors that are present in the gas. When integrated into a waste incineration plant, this device can also be used to recover the sensible heat in the flue gas and provide preheated combustion air.

During the previous year, a computer model was developed for a pebble-bed regenerator, and this model was used to size a regenerator for DIAL's combustion test stand. This computer model was used to size a pebble-bed regenerator for DIAL's combustion test stand. Our calculations indicate that this design will quickly cool the combustion

products through the critical dioxin formation temperature range--with a mean residence time of 0.6 to 0.7 seconds. Thus, this regenerator design should provide effective dioxin control.

During the current year, we will build and test this device on DIAL's combustion test facility. With a newly designed and built piece of equipment, testing should proceed incrementally, at each step verifying that the equipment performs according to design. The test sequence will proceed as follows: First, cold flow tests will be performed with no combustion to verify that the flow switching valves work properly and that our control system is sequencing the valves properly. Then, hot testing will begin. These tests will be performed to verify the correct operation of the system, that the flow switching valves work at the high temperatures for which they were designed, and that the pebble beds cool the combustion gases as they should. During this phase of testing, the pebble beds will be instrumented with thermocouples to measure the inlet and outlet gas temperatures, as well as temperatures inside the pebble bed at selected locations. The flow rates of gases through the beds will be measured. Also, the pressure drop across each bed will be measured.

These results will verify proper operation of the regenerator. The temperature measurements will be compared to the predictions of our model, and we hope that this comparison will validate the model. Also, the temperature measurements will verify that the desired quenching rate has been achieved.

The ultimate objective of this test program will be to demonstrate that the degree of quenching produced by the pebble bed is effective in reducing dioxin emission. To do this, we would like to perform a series of tests on DIAL's combustion test stand, injecting dioxin precursors upstream, and measuring dioxin levels downstream.

We intend that the dioxin level downstream of the regenerator will be measured and compared to the control -- the same test facility

without the regenerator. We would, of course, take care that the combustion parameters, such as the fuel/air ratio, were the same in both cases. DIAL maintains an in-house capability to perform dioxin measurements using EPA Method 23.

However, we must point out that there is currently some uncertainty about our permitting to carry out tests of this nature. Once this situation is resolved, then a detailed test plan for the dioxin testing will be written before the start of these tests and submitted to the Task Monitor for approval.

After the computer model has been validated by experiment, and we have verified that the rate of quenching is effective in reducing dioxin emissions, the validated computer model will be used to assess various approaches to scaling up. Maximum pebble bed size will be determined. Multiple regenerator configurations will also be studied as a possible approach to large scale operation.

Work Accomplished

Detailed design of the prototype has been completed. Shop drawings have been prepared. Materials and supplies have been ordered. Fabrication is underway in DIAL's shop facility.

Work Planned

The prototype will be completed, installed in DIAL's combustion test stand, and tested, as outlined in the introduction.

References

11. Kari Tuppurainen, et al., 1998. Formation of PCDDs and PCDFs in municipal waste incineration and its inhibition mechanisms: a review. *Chemosphere*, 36:7:1493-1511.

12. F.W. Karasek and L.C. Dickson.1987. Model studies of polychlorinated dibenzo-*p*-dioxin formation during municipal refuse incineration. *Science,* 237:754-756.

13. E.R. Altwicker, et al. 1990. Polychlorinated dioxin/furan formation in incinerator. *Hazardous Waste and Hazardous Materials,* 7:1.

14. J.J. Santoleri and M.L. Budin. May 1998. The impact of thermal oxidation quench systems on dioxin formation. IT3 Conference: International Conference on Incineration and Thermal Treatment Technologies, Salt Lake City, Utah.

Transportable Calibration Test Stand for Diagnostic Instrumentation

R. ArunKumar

Introduction

With the advent of modern diagnostic techniques for continuous emission monitors (CEM) and process monitors (PM), a need has evolved for the development of a bench-scale test train, which can be used for process simulation as well as for calibration of such instrumentation. The application of some of these instruments is limited by the availability of calibration streams, especially for low concentrations. In this task we aim to construct a versatile test bed that will be able to provide a test bed for calibration of optical diagnostic instrumentation over a range of temperature and concentration levels, for both combustion and non-combustion applications.

The system, as shown in Figure 10, is comprised of air flow, fuel flow, and dopant delivery streams. The air delivery system contains a pressure regulator, followed by a thermal mass flow measurement and control system, and an electric air heater. A dopant solution is deliv-

ered to a nebulizer or acoustic atomizer, which injects it as a fine mist of droplets into the throat of a venturi in the air delivery system. Propane is regulated, and its flow is controlled by a similar thermal mass flow meter/controller and injected into the throat of a second venturi in the air delivery system. The throat of a venturi provides a convenient place for injection of secondary streams, providing a lower pressure and also a smaller cross-section for more uniform dispersion. This combustible air stream is then ignited using a spark plug in the burner. The burner itself consists of a short water-cooled section followed by a hotter uncooled tube to maintain flame stability. The test bed will be instrumented for data acquisition and safety considerations.

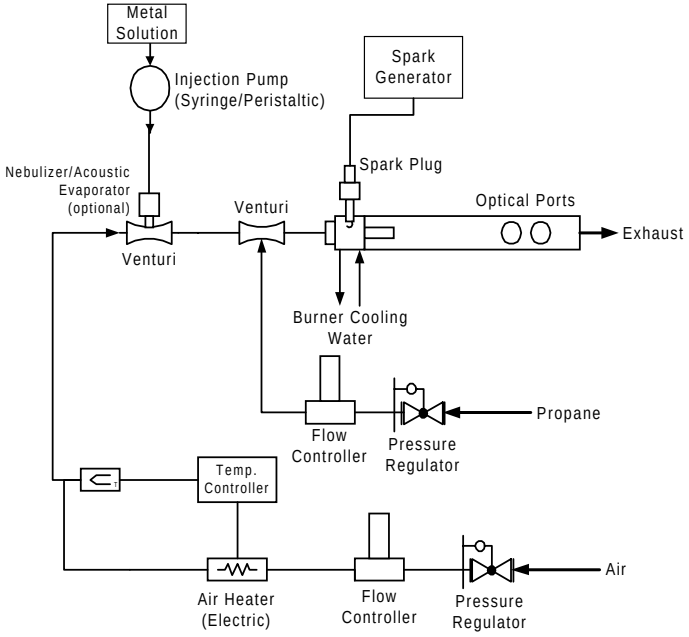

FIGURE 10. Schematic of the transportable calibration test stand for diagnostic instrumentation.

Work Accomplished

We have assembled the basic elements of the system which include the mass flow controllers for air and propane as well as an air pre-heater. The air exit temperature can be varied using the heater controller. Currently the LIBS system is making preliminary measurements in a 2-in. diameter pipe which is fed by the system. The whole system has been mounted on a 2 ft by 4 ft table with the pre-heater and mass controllers on a plate at the base of the table.

Work on the system is progressing satisfactorily and results from preliminary measurements should be available by the end of the next quarter.

Work Planned

In the next quarter, more LIBS measurements on the system are planned. We also will construct the burner and accompanying ignition system to complete the high temperature envelope of the combustion train.

Evaluation and Performance Enhancement of a Submerged Bed Scrubber

R. ArunKumar and M.J. Plodinec

Introduction

Submerged bed scrubbers (SBS) were originally developed by PNNL for treatment of off-gas from nuclear reactors. They have been proposed for use on the cleanup systems for scrubbing off-gases from liquid-fed ceramic melters used to vitrify high level waste, and from

other thermal processes. Submerged bed scrubbers serve dual purposes in that they act as a quench for high temperature exhaust gas and also remove at least 90% of the airborne particulate matter. These scrubbers are, however, susceptible to certain kinds of problems including poor gas distribution, gas surging, channeling and bumping. In this task, we propose to add a better gas distribution system under the SBS as well as replace the conventional spherical bed media with an engineered aggregate produced by Ushers, Inc. This "tetrajack" material more efficiently fills the bed volume than spheres (> 90% fill), and forces the gas stream to follow a tortuous path through the SBS.

Figure 11 shows a scale model of the West Valley SBS that will be constructed. It is primarily split into two parts, the gas distribution section and the scrubber bed section. Constructed of clear acrylic, the dual section assembly will allow us to observe, as well as readily test, different configurations of the gas distribution system.

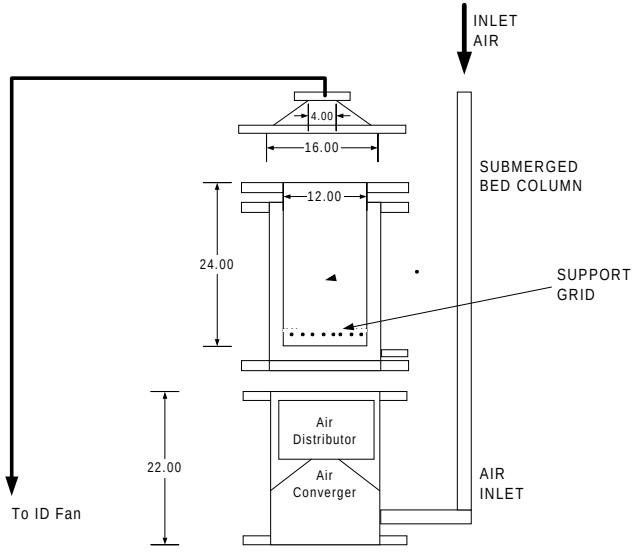

FIGURE 11. Scale model of West Valley submerged bed scrubber.

Operation of the test bed without modification will be performed first to develop base line performance data. The gas distribution in the bed will be observed visually, as will gas surging through the system. If needed, a positive air pressure delivery system can also be used to study gas distribution. Flow stability and surge parameters can be detected using differential pressure sensors. The first aspect of the testing will be to ensure that a uniform distribution of the gas is obtained under the submerged bed using a positive pressure feed system. This will be followed by testing using an induced draft fan, where surge effects can be determined and minimized. EPA measurements to determine particulate retention will be completed in the final stage of the testing. Capture of fine particulate material (talc or titania particles) and of simulated semi-volatile material (Cs salt) will be monitored, as will SBS operating parameters (e.g., flow rate, pressure drop).

At this point, the system will be cleaned, and the spherical bed material will be replaced by Ushers proprietary material. The base line testing will be repeated to evaluate the performance of this material. Then, the SBS model will be disassembled, and a flow distribution system will be inserted and tested with conventional (spherical) bed material. The same parameters will be monitored and evaluated.

Work Accomplished

Engineering drawings of the system have been completed, and we are in the process of ordering Plexiglas piping to construct the test bed. Spherical media for the submerged bed is also being ordered and the tetrajack material for the testing has been acquired.

Work Planned

The next quarter will primarily be devoted to the assembly and installation of the scrubber, which includes hook up to an induced

draft fan/force feed air supply. Initial testing on the system should also have begun.

TASK 3

Waste Treatment and D&D Support: Process Monitoring and Control

Dioxin and PCB Studies

C. Waggoner

Introduction

Selected congeners of the families of dioxins and furans (D/F) are potentially some of the most carcinogenic compounds known to exist. Recognition of the potential risk to the U. S. population spurred the conduction of a national inventory of D/F sources. A significant outcome of this initiative has been the establishment of a strategy to reduce emissions in a targeted fashion. One of the centerpieces of the D/F reduction strategy is the maximum achievable control technology (MACT) standard just issued for hazardous waste combustors (HWC). Each of the DOE hazardous or mixed waste incinerators falls subject to this new standard, and there are stringent emission levels that will need to be met in the near future.

The 0.2 ng/dsm^3 emission standard called for under the HWC-MACT stresses the technical limits of operational control and emissions testing. Uncertainties associated with US EPA reference method stack sampling accuracy and method quantification limits for the 17 D/F congeners that have non-zero toxicity equivalence factors

invite skeptical review of the measurements that will be made by facilities to demonstrate compliance with this new standard.

Of the six needs listed on the DOE EM-Needs web page related to dioxin/furan problems, three (ID-3.2.32, ID-S.1.02, and SR00-1021) recognize the lack of knowledge associated with the specific locus of D/F formation, the distribution of D/F congeners between adsorbed and gaseous phases at temperature, and/or the behavior of these classes of compounds in the sampling train. This lack of knowledge is an impediment to minimizing emissions by process control or design/operation of pollution control devices. Additionally, a much fuller understanding of the phase behavior in off-gases is essential to development of a functional continuous emission monitor or verifying the accuracy of extractive sampling methodologies. Finally, a clearer picture of the gas phase chemistry is the best hope of identifying a dependable analytical surrogate, if one exists.

Intensive research has been undertaken throughout the past two decades to gain a more complete understanding of the mechanism(s) of dioxin/furan formation in combustion processes. The majority of controlled mechanistic studies of D/F formation tend to be carried out using benchtop and micro-scale apparati. A significant body of data has also been accumulated from off-gas samples collected from solid waste incinerators and industrial processes. However, the large number of variables associated with fuel feed and operational history of incinerators makes it difficult to extrapolate from bench to full scale. A series of studies is proposed to take advantage of bench scale results and, in a two stage manner, extend these investigations to pilot scale.

The primary focus of this effort will be to determine the behavior of D/Fs associated with fly ash particulates in an isothermal off-gas environment for the temperature range of 300 to 800ºF. This will include analysis of samples for D/F homologues to determine the

extent of formation, destruction, and dechlorination under test conditions.

All of the results from these investigations will be utilized, along with literature information, in the initial development and evaluation of a hybrid artificial intelligence system (combination neural network-expert system) to project D/F formation, identify areas of needed research, and search for analytical surrogates.

Work Accomplished

During the first quarter of this fiscal year, our efforts have been directed toward:

- assembling materials necessary for development of the small scale test stand;
- reviewing the literature to develop a database of information to be used in formulation of the artificial intelligence (AI) software; and
- identifying and securing the commercial AI software to be employed in this study.

Materials needed for the test stand were ordered and nearly everything has arrived. Stainless tubing to be used for the isothermal reaction tube was damaged in shipment and is in the process of being replaced. Thermocouples, mass flow controllers, fittings, data access hardware, and structural steel are on hand. Raw materials needed for fabrication of the impactors are also in stock. Fabrication will begin as soon as it can be scheduled, once the damaged tubing has been replaced.

A more thorough literature review has been conducted and a database of information to be used in AI development is underway. The commercial AI software to be employed has been identified and ordered.

Work Planned

During the next quarter, the small scale test stand will be fabricated and brought to operational status. System functionality and characterization studies will begin. The modified impactor-based off-gas sampling train will also be built with characterization studies and preliminary evaluation relative to the EPA Reference Method M23A initiated.

The database of literature values will be completed and employed to finalize the test plans for initial experiments looking at the distribution of D/Fs in the solid and vapor phase as a function of temperature. These data will also be used in the initial formulation and evaluation of the AI software that is a part of this study.

References

15. K.L. Froese and O. Hutzinger. 1997. *Environmental Science Technology* 31:542-547.

16. A. Addink, H.A.J. Govers and K. Olie. 1998. *Environmental Science Technology,* 32:1888-93.

17. P.M. Lemieux and J.V. Ryan. 1998. *Waste Management*, 18:361-370.

18. P.H. Taylor and B. Dellinger. 1999. *Journal of Analytical and Applied Pyrolysis*, 49:9-29.

19. F. Iino, T. Imagawa, M. Takeuchi and M. Sadakata. 1999. *Environmental Science Technology*, 33:1038-43.

On-line Multi-spectral Imaging of Thermal Treatment Processes

D. L. Monts and Yi Su

Introduction

Purpose

Many of the DOE waste streams, particularly those currently stored in steel barrels, are poorly characterized or even uncharacterized. Given the variety of contents that can dramatically vary from barrel to barrel, it is necessary for thermal treatment systems (TTS) to quickly change operating parameters and/or implement divert-and-treat measures when specific species of environmental concern (such as mercury) are suddenly introduced into the TTS. It is desirable to monitor species of concern inside the primary TTS chamber in order to provide the maximum possible response time and because concentrations will be higher here and, hence, easier to detect.

Digital images contain a wealth of information that, if extracted, could be of immense value for monitoring/controlling a process. Imaging spectroscopy combines conventional imaging, spectroscopy, and radiometry technologies to produce images for which a spectral signature is associated with each spatial resolution element (pixel). The emphasis of this project is on extending previous work to include extraction of information on concentrations, concentration distributions, and other parameters of use for process control of thermal treatment systems of interest to DOE. Using visualization and neural network techniques, the information can be presented in such a manner as to assist decision-making. Extraction of information from the primary thermal treatment chamber will provide sufficient time for operational parameters to be changed to maintain optimum operational performance and/or to allow divert-and-treat actions to be

taken for species of environmental concern. Previous work at DIAL has shown the utility of digital images for visual display of thermal distribution contours and for determination of average temperatures.

Methodology

Combining spectral and spatial analyses allows application of imaging technology to species characterization and detection inside primary chambers of thermal treatment sources for mixed hazardous waste processing. We are developing a spectral imaging system by combining a charge-coupled device (CCD) camera with narrowband optical filters. For the proof-of-concept experiments, a series of narrowband interference filters are utilized to obtain images of the combustion chamber at wavelengths characteristic of selected metal species. Subsequent efforts will employ an acousto-optic tunable filter (AOTF) in order to significantly increase the number of different wavelengths (and hence species) that can be monitored by the imaging system. The digital images are analyzed using commercially available software that is being modified to meet the needs of this project. We are also developing the methodology to calibrate the spectral imaging system. Analysis of the spectral images will be combined with neural network techniques in order to provide facility operators with practical information on a time-scale short enough to enable process control decisions to be made.

Work Accomplished

Previously, we assembled a prototype spectral imaging system by using narrowband interference filters with CCD cameras and successfully demonstrated proof-of-concept for application of spectral imaging to quantitative detection of metal species in a practical thermal treatment system. After completion of the proof-of-concept experiments, we began working toward our next milestone, purchasing essential equipment and assembling the imaging spectrometry system for multi-species detection. The ultraviolet acousto-optic tunable fil-

ter (UV AOTF) has been ordered with delivery expected in July. Progress on the hardware portion of our development effort is dependent upon receipt of the UV AOTF unit.

Our efforts to further refine and improve our data analysis computer subroutines continued. Neural network development efforts and future DIAL test stand data collection efforts were coordinated. The neural network efforts are now being directed toward determination of the concentration of a single species in near real time from spectral images of thermal treatment.

Work Planned

When the UV AOTF arrives during the next reporting period, we will assemble the multi-species system and begin optimization of the system. We will begin the next round of DIAL test stand experiments, employing several species. Selection of species is based on (1) the presence of strong, spectrally isolated emission in regions of high detection sensitivity and (2) the ability to obtain permission to introduce the selected species into the DIAL test stand at concentrations that will not interfere with simultaneous or subsequent experiments performed by other DIAL research teams. Species currently under consideration for the next round of DIAL test stand experiments include, but are not limited to, Li, Mn and Co.

Acronyms

AOTF	acousto-optic tunable filter
CCD	charge-coupled device
DIAL	Diagnostic Instrumentation and Analysis Laboratory
TTS	thermal treatment systems
UV	ultraviolet

On-Line Monitor for Gall Layer Detection

Gene Ramsey

Introduction

Work has been performed to design, test and develop a monitor for detecting the presence of sulfate salts (gall) on the surface of a glassy melt. This project is intended to deliver an on-line prototype for use with waste vitrification systems.

The initial period of testing has been primarily devoted to room-temperature glass/gall surrogates. These test indicate that honey (glass) and methanol (gall) are acceptable surrogates. The detection of methanol layers on a honey surface can be performed with visible light techniques (at room temperature) and waves produced by agitation, such as affected by bubbling the melt, appear to greatly enhance to potential for gall layer detection.

Two room temperature systems have been constructed. Data has been taken during a variety of test conditions. It is likely that a gall surface may be detected by examination around a region a turbulence and created by a melt bubbler.

Work Accomplished

Two test systems have been constructed. The most advanced system mimics a waste furnace bubbler and allows controlled methanol (gall) addition.

Test apparatus images captured on CD format. Tests performed on varying depth of methanol to determine likely sensitivity of technique.

A high temperature furnace is being constructed which allows gall material addition and optical access.

Detection of the methanol layers by optical methods occurs at layer depths on the order of 0.5 to 1.0 millimeter.

Work Planned

Low temperature furnace operations will begin within the month. The high temperature furnace will be operational within one week of receipt of final parts.

Most of the experimental efforts during July were centered on salt well pumping experiments under different heat transfer conditions and at different surrogate flow rates (Reynolds numbers). The time needed to form a solid plug increased with increasing cooling and decreased with increasing Reynolds number at constant heat transfer. In the case of the highest Reynolds number yet investigated (~300) plug formation took over an hour. The pressure profile indicated some increases and decreases presumably associated with the formation and distribution of small sections of gelled material within the channel. The corresponding pressure profile at the lowest Reynolds number (~180) formed within four minutes. Once the plug has been established within a section of pipe little time is needed to completely plug the channel downstream of the original plug location. Avenues for modeling the experimental data are under investigation. Information on the problems observed when salt well pumping the liquor from Hanford tank 241-SX-104 was received from Jim Jewett at Hanford. Further discussions are in progress to represent the laboratory data to the best effect possible for the operators at the site.

The new dual-processor workstation was received and simulations on plug formation from slurries (particle deposition) are continuing. Parametric studies were performed using the CFD model on a small-scale pipeline transfer. The main variable was the flow veloc-

ity (flow rate). The FIU simulant C was used as a model for the slurry and consisted of a carrier fluid with a density of 1.005 g/ml and a volume fraction of 92.4% and solid particles of two sizes. The sizes of the particles were 45 and 220 microns with a density of 3.147 g/ml. The volume fraction of the smaller particles was 2.9% and 4.7% for the larger ones. The simulations showed that the amount of solid particles deposited on the bottom of the transfer pipe increases rapidly as the flow initial velocity at the pipe entrance was decreased. This behavior causes a sharp reduction in the flow rate and eventually the formation of a plug in the pipeline. More studies on larger scale transfers are being performed.

Most of the experimental efforts during July were centered on salt well pumping experiments under different heat transfer conditions and at different surrogate flow rates (Reynolds numbers). The time needed to form a solid plug increased with increasing cooling and decreased with increasing Reynolds number at constant heat transfer. In the case of the highest Reynolds number yet investigated (~300) plug formation took over an hour. The pressure profile indicated some increases and decreases presumably associated with the formation and distribution of small sections of gelled material within the channel. The corresponding pressure profile at the lowest Reynolds number (~180) formed within four minutes. Once the plug has been established within a section of pipe little time is needed to completely plug the channel downstream of the original plug location. Avenues for modeling the experimental data are under investigation. Information on the problems observed when salt well pumping the liquor from Hanford tank 241-SX-104 was received from Jim Jewett at Hanford. Further discussions are in progress to represent the laboratory data to the best effect possible for the operators at the site.

The new dual-processor workstation was received and simulations on plug formation from slurries (particle deposition) are continuing. Parametric studies were performed using the CFD model on a small-scale pipeline transfer. The main variable was the flow veloc-

ity (flow rate). The FIU simulant C was used as a model for the slurry and consisted of a carrier fluid with a density of 1.005 g/ml and a volume fraction of 92.4% and solid particles of two sizes. The sizes of the particles were 45 and 220 microns with a density of 3.147 g/ml. The volume fraction of the smaller particles was 2.9% and 4.7% for the larger ones. The simulations showed that the amount of solid particles deposited on the bottom of the transfer pipe increases rapidly as the flow initial velocity at the pipe entrance was decreased. This behavior causes a sharp reduction in the flow rate and eventually the formation of a plug in the pipeline. More studies on larger scale transfers are being performed.

Imaging Instrumentation Application and Development: Thermal Imaging

Ping-Rey Jang and Gary Boudreaux

The main thrust of this task is to develop and maintain DIAL's on-line thermal imaging system and the development of imaging instrumentation using the Fourier transform profilometry (FTP) technique.

Introduction

DIAL's thermal imaging system has been used successfully to monitor the thermal distribution on various types of waste treatment furnaces. The viscosity of the melt, and volatility of species in the melt, is a function of the temperature and composition of the melt. Thus, it is essential to measure the melt temperature during the treatment process. It is also critical that facility operators are able to view the surface of the melt bath from the temperature distribution point of view, so that appropriate on-line process control/adjustment procedures can be justified.

Temperature measurement is based on Planck's radiation law assuming a graybody radiator. An ideal radiator, called a blackbody, will have a hemispherical spectral emissive power given by Planck's law,

$$e_B(\lambda,T) = C_1\lambda^{-5}/[exp(C_2/\lambda T)-1], \quad \textbf{(EQ 1)}$$

where e_B is the emissive power, λ is the wavelength, T is the absolute temperature of the blackbody, C_1 and C_2 are constants. The temperature is determined by measuring the spectral emittance of a blackbody at any wavelength. In reality, most radiators are not blackbodies and so have a lower emissive power at the same temperature. The ratio for the spectral emissive power of an object to that of a blackbody at the same temperature is the object's emissivity, ε_l. The spectral emissivity, which may have values between zero and one, will depend upon the object's physical properties and may be a function of wavelength. The spectral emissive power of any radiator is given by

$$e_B(\lambda,T) = \varepsilon_l C_1\lambda^{-5}/[exp(C_2/\lambda T)-1]. \quad \textbf{(EQ 2)}$$

Work Performed

The system development objectives of this technical task during this period were to enhance the image system software with adjustable emissivity plug-in values. With emissivity values obtained from DIAL’s two-color pyrometer (TCP) system, the accuracy of the temperature within a target surface can be greatly improved.

The effect of the target surface emissivity value in Planck’s radiation law was studied. As shown in Table 4, it is noted that the lower the surface emissivity the larger the percent error, and the temperature correction by the target surface emissivity becomes more significant.

The software development for the user adjustable emissivity input control modules has been completed.

TABLE 4. Temperatures affected by the target surface emissivity in Planck's function assuming apparent blackbody temperature = 1500˚C with 0.9 m as effective wavelength.

Emissivity (ε_λ)	Corrected Temp. (˚C)	Δ T (˚C)	Percent Error (%)
1	1500.0	0.0	0.0
0.9	1521.0	21.0	1.4
0.8	1545.0	45.0	2.9
0.7	1573.0	73.0	4.6
0.6	1606.5	106.5	6.6
0.5	1647.7	147.7	9.0
0.4	1700.6	200.6	11.8
0.3	1773.2	273.2	15.4
0.2	1885.2	385.2	20.4
0.1	2107.8	607.8	28.8

Work Planned

We will continue to work with the integration of these software modules and the thermal imaging system software. Testing for the complete system against a standard temperature calibration source will follow.

Reference

20. P.R. Jang, R.D. Benton and R.L. Cook. June 1994. Some observations on the spectral response in pyrometry. AIAA 94-2445.

Imaging Instrumentation Application and Development: Profilometry

Introduction

DIAL's profilometry system has been developed to measure surface profiles before and after a surface has been changed or scabbed. By utilizing Fourier transform profilometry (FTP), an image processing technique, the volume and depth of material removed from a surface can be calculated.

The technique for the decontamination and decommissioning (D&D) of concrete structures within the Department of Energy and the nuclear industry is to remove a specific amount of material from the surface using a technique known as scabbling. The profilometry system developed at DIAL uses a structured light pattern projected onto a surface, and by analyzing the distortions of the pattern using a digital camera, the shape of the object can be determined. As a wall removal monitor, the technique uses a projected light pattern that is cast onto the surface of the wall. An image is captured before work is started on the surface, then a second image is captured after the work has been completed. Processing the two images yields the new surface profile relative to the original surface. Volume and depth of material removed from the surface can be calculated. The development of this system addresses DOE-EM and nuclear industry needs in the decontamination and decommissioning (D&D) of concrete structures.

Work Performed

In order to improve the system flexibility in software development for imaging instrumentation, an ANSI C-based development platform has ben adopted. This transfer also includes replacing the still digital camera with a B/W digital video camera. An image acqui-

sition board has been added to increase the image acquisition rate to 30 frames per second.

For the projection system to work under bright ambient light conditions, a 1-KW Xe strobe light fixture has been utilized for stronger light projection intensity. Both computer controls and manual controls for the synchronization between the camera and the strobe light fixture have been completed. A software module for image acquisition has been developed. This module allows the user to acquire an image as the Xe strobe light reaches peak intensity.

Work Planned

Further improvements on image acquisition, analysis and presentation in the new ANSI C-based development platform will be continued. To compare the Xe strobe light's spectral intensity at 823 nm with the sun light, a spectrometer will be utilized to measure both light sources.

Reference

21. M.E. Henderson and R.D. Costley. June 1998. Wall removal monitor. DIAL Technical Memo FTP 698.

Saltcake Dissolution

R. K Toghiani, J. S. Lindner and H. Al Habbash

Introduction

This project is a continuation of the work previously reported on the dissolution of Hanford waste saltcakes. A main portion of the work is to continually validate and upgrade a thermodynamic equilib-

rium model, the Environmental Simulation Program (ESP) as applied to the Hanford wastes. Toward this end a number of significant accomplishments have been reported previously.[22-26] These include the evaluation of the code for the dissolution of saltcakes varying in composition through a comparison of model predictions with experimental results on core samples performed at the site, the use of the model to aid in the development of remediation strategies for Hanford tank 241-SY-101, an evaluation of data preprocessing, and the experimental determination of the solubility of natrophosphate, a double salt observed in the tank wastes.

A main focus is in bolstering the predictions of the code through comparison with experimental data and with other thermodynamic models such as SOLGASMIX. Accurate data called by the model are an essential requirement for quantitative code predictions; however, it must be noted that evaluation of the thermodynamic interactions between all of the species existing in the waste streams is not possible. The path, therefore, has been to concentrate on those anions such as nitrate, nitrite, hydroxide, sulfate, phosphate, fluoride, oxalate, carbonate, and cations, sodium, aluminum, calcium, nickel, uranium, etc., and the associated solids from these species that comprise the majority of the waste composition. Once assured that the code predictions accurately reflect the thermodynamics of these systems, it becomes possible to further upgrade the model to include other species of considerably lower concentration. The project is divided into three tasks as summarized below.

Task 1. Comparison of ESP to other thermodynamic equilibrium codes. The model has been shown to provide agreement with literature data for the solid liquid equilibrium behavior of many of the saltcake constituents at both high and low ionic strengths. Nonetheless questions will remain on the application of the model to situations where the ionic strength is high owing to the extrapolation of fundamental electrolyte theory to regions of high ionic strength. Theoretical calculations for the most prevalent solid in the waste, sodium nitrate, will be

performed at high ionic strength and compared to an alternate model developed by M. Ally at ORNL. Comparisons with the SOLGASMIX model, in collaboration with C. F. Weber (ORNL) will be performed for the sodium-fluoride-sulfate system. Companion solubility experiments will be made on this system to improve the ESP database (Task 3).

Task 2. Comparison of ESP predictions to saltcake dissolution experiments. Previous work has characterized saltcakes with roughly four typical compositions as anticipated in the Hanford tank wastes. These studies have indicated that ESP can be used to predict the dissolution behavior of the majority of the solids present. An exhaustive search for other types of saltcake compositions was conducted recently by D. L Herting of NHC resulting in the identification of two additional tanks with different composition distributions. A sample from tank TX-113 will be evaluated this year. In addition, recent interest in pretreatment and retrieval operations has indicated that there may be some concern when supernates from different waste streams are combined. ESP will be used with the predicted supernates from some of the previous saltcake dissolution studies to examine the propensity of solids formation under expected operating conditions. Predictions will be compared with on-going experimental work at the site.

A conference on the dissolution of saltcake will be organized and this forum will provide for extended discussions on the progress and results of the work and on future programmatic directions. Reports on the saltcake dissolution studies and on the outcomes of the saltcake dissolution conference will be provided.

Task 3. Improvements and user documentation for the ESP model. Some deficiencies have been shown to exist within the ESP databanks.[22] Of high interest is the determination of solubility data for double salts. Solubility studies for Na_3FSO_4 will be conducted and compared to the results of the prior literature and the calculations performed in Task 1. Additional studies on the extent of hydration as a function of ionic

strength will be performed for Na_2CO_3 and Na_3PO_4.[27] Experiments are also planned for NaF at elevated ionic strength and in the presence of $NaNO_3$.

Considerable effort has been expanded in learning the most appropriate ways in which to develop and run ESP simulations. These will be documented and forwarded to customers at Hanford for incorporation in the *ESP User Manual.*

Work Accomplished

Results and Discussion

Task 1 focuses on the comparison of the ESP thermodynamic predictions with calculations from other thermodynamic codes and with published literature data for select chemical systems. During FY 99, comparisons between ESP and SOLGASMIX were conducted for the sodium-fluoride-phosphate double salt solubility. Comparison of dissolution experimental measurements with ESP predictions for saltcakes from the Hanford site indicated that discrepancies existed between experiment and predictions at low levels of dilution. The reason for these discrepancies was hypothesized to be the result of either: 1) inadequacies in the fundamental thermodynamic data for select sodium double salts, which are present in the solid phase at low levels of dilution and undergo complete dissolution at higher levels of dilution; or 2) inadequacies in the ESP code with respect to representation of behavior for high ionic strength systems. In an effort to uncover the cause of the discrepancies, ESP was used to predict the vapor pressure over a sodium nitrate solution at 25˚C, 100˚C and 125˚C. Similar calculations were completed for the aqueous sodium nitrate system by M. Ally of ORNL using a lattice model to predict the thermodynamic behavior.[28] Both sets of calculations were compared to literature data for the vapor pressure over sodium nitrate solutions from the *International Critical Tables.* Figure 12 provides a

comparison of the calculations and experimental literature data at 25˚C. This comparison indicates that the discrepancies realized in the modeling of saltcake dissolution experiments at low dilution levels are primarily due to inadequacies in the fundamental thermodynamic data for the sodium double salts rather than a result of inadequacies in the ESP calculations at high ionic strength. The ESP predictions agree well with both the experimental data as well as with the predictions of M. Ally. At both 100˚C and 125˚C, similar behavior was observed. In much of the saltcake waste at Hanford, sodium nitrate is a dominant species and ESP's predictive capabilities with respect to this species under conditions realized in the tank waste at Hanford has been verified through these comparative calculations.

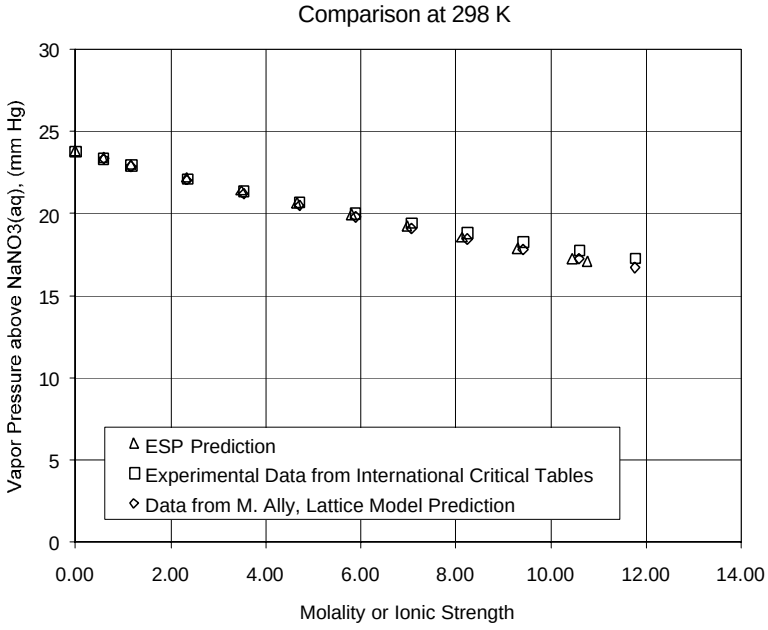

FIGURE 12. Vapor pressure over aqueous sodium nitrate solutions at 25˚C.

Task 2 focuses on the use of ESP to model the saltcake dissolution experiments conducted by Herting on actual Hanford waste from

select tanks. The saltcake chosen for FY 00 studies is from tank TX-113 and contains significant amounts of a number of anions. Table 5 provides a summary of the saltcakes examined during the past three fiscal years at Hanford. These tanks have been the focus of ESP modeling efforts at MSU. The saltcake from TX-113 contains significantly more sulfate and carbonate than the other saltcakes examined as well as elevated levels of fluoride and phosphate. These anions combine with sodium to form a variety of double salts including sodium-fluoride-phosphate (natrophosphate, $Na_7F(PO_4)_2 \cdot 19H_2O$) and sodium-fluoride-sulfate (burkeite, Na_3FSO_4). The original saltcake from TX-113 has little to no liquid phase. Identification of the solids present in the original saltcake is one of Herting's FY 00 tasks.

TABLE 5. Major constituents in saltcakes examined (weight % of sample).[a]

	TANK				
	TX 113	**BY 102**	**BY 106**	**A 101**	**S102**
H_20	12.90	26.51	14.7	31.2	(5.0)
Al^{+3}	0.32	1.65	1.58	2.39	0.67
Ca^{+2}	0.02	0.043	0.013	0.008	
Cr^{+3}	0.04	0.199	0.113	0.17	0.12
Fe^{+3}	0.03	0.053	0.019	0.014	(0.03)
K^+	0.03		0.243	0.31	0.07
Mn^{+2}		0.024			
Na^+	30.55	27.75	24.98	21.20	23.0
Ni^{+2}		0.026	0.006		
P		0.998	0.078	0.14	0.18
Si	0.04	0.072	0.017	0.027	0.03
S		2.03	0.447	0.8	0.13
U	0.15	0.064	0.019	0.034	

[a] Data from Ref. 29,30; ( ) represents questionable result
[b] Report as CO_3^{2-}
[c] Calculated
* Total inorganic carbon (CO_3^{2-}/5)

TABLE 5. Major constituents in saltcakes examined (weight % of sample).[a]

	TANK				
	TX 113	**BY 102**	**BY 106**	**A 101**	**S102**
TIC*	15.07[b]	4.13	1.43	1.81	0.59
$C_2O_4^{-2}$	0.04	1.99	1.26	1.35	0.17
Cl^{-1}	0.06	0.11	0.16	0.41	0.16
F^{-1}	0.76[c]	1.17	0.62	0.069	<0.02
NO_2^{-1}	0.26	1.85	2.71	7.43	2.04
NO_3^{-1}	19.12	10.92	40.54	12.6	53.7
OH^{-1}	0.30	1.09	1.14	2.1	0.42
PO_4^{-3}	3.75	(0.06)	0.34	0.44	0.56
SO_4^{-2}	16.67	5.12	1.16	2.41	0.38
TOC		0.63	0.48	0.56	0.17

[a] Data from Ref. 29,30; ( ) represents questionable result
[b] Report as CO_3^{2-}
[c] Calculated
* Total inorganic carbon (CO_3^{2-}/5)

During FY 99, a recommended approach was developed for charge reconciliation of laboratory data. These laboratory data are used as input to the ESP program, but often exhibit a net charge imbalance. The proration method (where the charge imbalance is distributed across either the cations or the anions) was recommended and an iterative procedure for tuning the density of the sample was recommended so that the generated molecular stream had the appropriate loading of the various cations and anions. This recommended approach worked well for three of the four saltcakes examined in earlier years. However, for the S-102 saltcake examined during FY 99 and for the TX-113 saltcake examined during FY 00, this recommended approach failed because of the extremely low initial water content. An alternate approach has been developed to handle the data pre-processing for the 'low-water content' saltcakes. In this alternate approach, sufficient diluent water is added to allow generation of a

molecular stream with ESP. This stream is then equilibrated with sufficient diluent to achieve a dilution of 300% by weight (3 grams of diluent per 1 gram of original saltcake). Since these saltcakes contain significant amounts of nitrate, the nitrate concentration at 300% dilution is used as a target value. The input density to the water analyzer program is adjusted until the predicted nitrate concentration agrees with the experimental value at 300% dilution. This method has been used to successfully pre-process the laboratory data for saltcakes from tanks S-102 and TX-113.

During FY 99, it was determined that adequate representation of the sodium carbonate system at higher ionic strengths was possible only with the inclusion of a specialized database, the Trona database, which provided additional fundamental thermodynamic data for this system. The need for this database was uncovered when simulations of the BY-102 saltcake were conducted and predicted anion concentrations were compared with experimental measurements from Herting's experiments. Tank BY-102 had the highest levels of carbonate of the four tanks studied in earlier years. Preliminary simulations for the TX-113 saltcake were conducted using the Public database and the Trona database. These preliminary results indicated the need for improved thermodynamic data for the sulfate species; in particular, sodium sulfate anhydrous, sodium sulfate decahydrate, and the sodium fluoride sulfate double salt. In Figure 13, predictions for sulfate anion (labeled 'Public + Trona') are shown along with the experimental measurements from the series dissolution tests of Herting for TX-113 saltcake. The ionic strength calculated by ESP at a dilution level of 50% is 24.4. The sulfate concentration predictions exhibit behavior typically of a species that is entirely found in the supernate, while the experimental data exhibit behavior typical of a species undergoing dissolution as diluent is added. This behavior is very similar to that exhibited by the carbonate anion in preliminary simulations for the BY-102 saltcake which led to the incorporation of the Trona database in order to adequately describe the carbonate behavior under high ionic strength conditions. Discussions with OLI personnel

identified a similar database, the Na2snacl database, for anhydrous sodium sulfate and sodium sulfate decahydrate. Anhydrous sodium sulfate had been identified in the solid phase of TX-113 saltcake by Herting, but was not initially predicted to be present in the solid phase by ESP. Incorporation of this database along with the Public and Trona databases significantly improved the predictive capabilities of ESP with respect to sulfate anion in the TX-113 saltcake. Anhydrous sodium sulfate was predicted to partition into the solid phase in agreement with experiment and the calculated ionic strength of the equilibrium supernate was significantly lowered (from 24.4 to 16.7 at a 50% dilution). These improved predictions are also plotted in Figure 13 and labeled as 'Public + Trona + Na2snacl'. Examination of saltcakes that contain a high percentage of one or more select anions allows identification of the need for specialized databases.

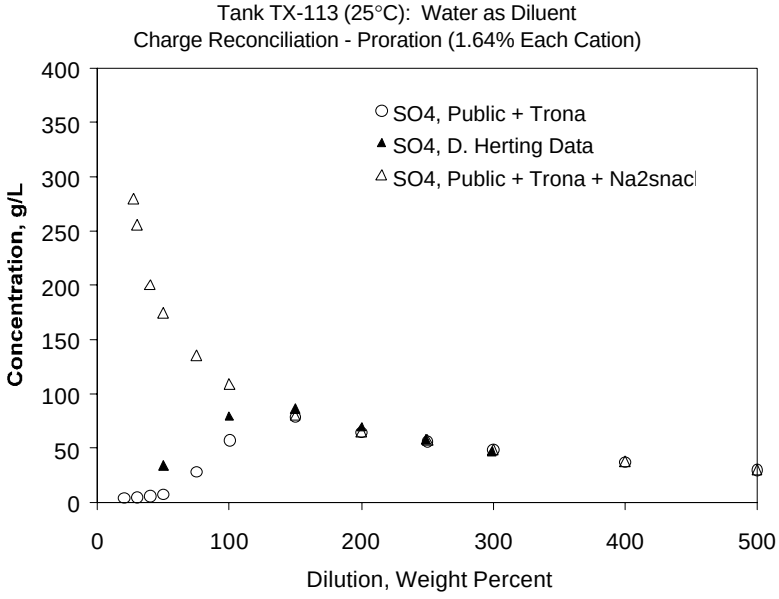

FIGURE 13. Comparison of predicted and experimental sulfate concentrations for Tank TX-113 saltcake.

Solids characterization efforts were conducted by Herting during FY 99 for the BY-102 saltcake. Anhydrous sodium sulfate was identified in the solid phase of the original saltcake as were sodium nitrate, sodium carbonate monohydrate, natrophosphate, and burkeite. This characterization study was driven by the need to compare ESP predictions of the solid phase with experimental data. In previous simulations of BY-102 saltcake, anhydrous sodium sulfate has not been predicted to be present in the solid phase. Simulation of the series dissolution test for BY-102 saltcake will be repeated using the combination of three databases (Public, Trona and Na2snacl) in an attempt to better reproduce the experimental solids characterization.

Task 3 focuses on improvements to the ESP databases and development of user documentation to facilitate the routine use of ESP as an operations planning tool at the Hanford site. During this quarter, significant progress was made in solubility measurements for the sodium-fluoride-phosphate and sodium-fluoride-sulfate systems. Experimental measurements for the solubility as a function of ionic strength and temperature are underway with solid phase characterization by polarized light microscopy. These data will then be supplied to OLI for incorporation into the ESP public databases to provide improved predictive capabilities for these double salts with the ESP code.

A strategy for data pre-processing of laboratory data for low-water content saltcakes was identified and tested with two saltcakes, TX-113 and S-102. This procedure will be fully documented so that personnel at the Hanford site can utilize the method.

Conclusions

Deficiencies in ESP's predictive capability have been traced to deficiencies in the fundamental thermodynamic data available for select species in the Public database. Use of ESP under conditions of high ionic strength has been examined through comparative calcula-

tions with a lattice model developed by Ally at ORNL. A method of data pre-processing of low-water content saltcakes has been developed. In modeling of series dissolution experiments, inclusion of specialized databases improves the representation of both carbonate and sulfate species.

Project Status

Improvements in the representation of sodium double salts, in particular, the fluoride-phosphate double salt and the fluoride-sulfate double salt, require the availability of additional equilibrium data at conditions comparable to those that exist in the Hanford site. Experimental measurements of the solubility envelopes for these double salts have been undertaken. These measurements, when incorporated into the ESP database, will provide for improved predictive capabilities for these systems.

Work Planned

Experimental results from the series dissolution tests conducted by Herting indicate that the various salts in the waste will dissolve at different levels of diluent addition. In an effort to model the staged retrieval which may be necessary at the Hanford site, Herting designed additional experiments for the FY 00 year entitled “Feed Stability” experiments. In these experiments, diluent is added in a sequential manner. After equilibration, the liquid phase is segregated and the liquid retrieved from each contact is stored in a cumulative receiver tank. The formation of solids in this cumulative receiver tank from these combined liquid streams could result in the formation of salts that could plug pipelines or cause other operational problems. ESP simulation of the feed stability experiments will provide predictions that can be compared to experimental data.

References

22. R.K. Toghiani, J.S. Lindner, C. Barfield and E.C. Beahm. 1998. *Saltcake Dissolution Modeling, FY 1998 Status Report.* DIAL-40395-TR98-1, Diagnostic Instrumentation and Analysis Laboratory, Mississippi State University, Mississippi State, MS.

23. R.K. Toghiani and J.S. Lindner. 1999. Saltcake Dissolution Modeling, FY 1999 Status Report. DIAL-40395-TR99-1, Diagnostic Instrumentation and Analysis Laboratory, Mississippi State University, Mississippi State, MS.

24. J.S. Lindner, R.K Toghiani and C. Barfield. August 1998. Thermodynamic Simulation of Tank 241-SY-101 Dissolution, Part 1: In Situ Crust Dissolution. DIAL 40395-TR98-1, Diagnostic Instrumentation and Analysis Laboratory, Mississippi State University, Mississippi State, MS.

25. J.S. Lindner and R.K Toghiani. October 1998. Thermodynamic Simulation of Tank 241-SY-101 Dissolution, Part 2: Supernate Transfer followed by In-Tank Dilution. DIAL 40395-TR98-1.2, Diagnostic Instrumentation and Analysis Laboratory, Mississippi State University, Mississippi State, MS.

26. J.S. Lindner and R.K Toghiani. April 1999. Thermodynamic Simulation of Tank 241-SY-101 Dissolution, Part 3: Crust Solids Dissolution Modeling and Associated Gas Release. DIAL 40395-TR98-1.3, Diagnostic Instrumentation and Analysis Laboratory, Mississippi State University, Mississippi State, MS.

27. D.L. Herting. October 1999. Personal communication.

28. M. Ally and J. Braunstein. 1996. Activity Coefficients in Concentrated Electrolytes: A Comparison of the Brunauer-Emmett-Teller (BET) Model With Experimental Values. *Fluid Phase Equilibria* 120:131.

29. D.L. Herting and D.W. Edmonson. September 1998. Saltcake Dissolution FY 1998 Status Report, HNF-3437, Rev. 0.

30. D.L. Herting, D.W. Edmonson, J.R. Smith, T.A. Hill, C.H. Delegard. September 1999. Saltcake Dissolution FY 1999 Status Report, HNF-5193, Rev. 0.

Feed Stability and Chemistry: Solids Formation

J. S. Lindner, H. Al-Habbash, and R. K. Toghiani

Introduction

Tank farm operations at Hanford include the interim stabilization program where the supernate and interstitial liquor in the single-shell tanks is reduced. Benefits from this process include the minimization of leakage from aging tanks, thereby limiting migration of waste into the soil, and the temporary reduction of waste within the tank. The process consists of jet-pumping the liquid in a given tank, obtained through a screen or salt well to a double-shell holding tank and then to an evaporator. Dilution water is added at the pump head. Recently, solids formation and plugging have been noted during transfers from tanks 241-SX-104, 241-U-103, and 241-BY-102.[31] The primary solid responsible for the plugs from the first two tank wastes has been tentatively assigned, through experiments conducted on the waste liquid in the laboratory, as $Na_3PO_4 \cdot 12H_2O$. The plug formed during salt well pumping of BY-102 was believed to arise from sodium carbonate.

Other solids may participate in the plug formation process and this will largely depend on the solid-liquid equilibrium of the species contained in the waste stream. Little information, aside from the laboratory screening experiments is known regarding the mechanisms of plug formation and, more importantly, the required change in pressure that would indicate the beginning of plug formation. From operations measured records, the time needed for a plug can be determined and by knowing the pressures and flow rates the approximate location of the plug can be estimated; however, prevention of inadvertent plugs may be possible based on a suitable engineering tool that will allow operators to tailor waste transfers.

Development of an engineering tool that can describe slurry transfers and salt well pumping is also an objective of this program. In the case of slurry transport experimental data is being obtained at Florida International University and information on solids behavior, size, and growth rates is being measured at AEA Technologies. A test loop for obtaining data on supernate transfers does not currently exist. The work described below focuses on the development, construction, and testing of a salt well pumping apparatus. The information will support current operations at Hanford and will provide the data needed to initiate model development activities associated with this program.

Results and Discussion

Salt Well Pumping Flow Loop

The salt well pumping flow rates at Hanford range from 0.4 to 5 gal/min. The supernate flows through nominal 3-in. mild steel pipe and can be diverted through junction boxes. Many portions of the transfer lines are heat-traced, however, the junction boxes that use either rigid or flexible insertion pipes (“jumpers”) may or may not be temperature controlled. Changes in waste temperature will effect flow properties through changes in the solid-liquid equilibria.

Development of a laboratory-scale test loop with 3-inch pipe and flow rates common to the actual operation was considered impractical. The initial configuration of the loop included a channel tube with shell heat exchangers. A Mathcad program was written to determine the diameter and length of the exchangers. For the calculations the viscosity of the waste stream was taken from the average ESP predictions for the supernate stream over the temperature range 15 - 60˚C. The heat capacity was determined from ESP enthalpy results (see below) and the thermal conductivity was assumed as that of water.

Comparison of the salt well pumping operation at the site with the laboratory test loop was based on the Reynolds number. Flow of waste supernate with a density of 1424 kg/m^3 and absolute viscosity of 4.16 cp at a rate of 0.132 m^3/hr (0.5 gpm) through a 7.62 x 10^{-2} m (3-inch) pipe corresponds to a Reynolds Number of 180. For the laboratory experiments it became convenient to employ a 6.35 x 10^{-3} m (0.25-inch) id stainless steel tube. ESP calculations on the surrogate stream provided a density of 1460 kg/m^3 and an average viscosity of 8 cp. The flow rate needed to match the flow conditions at the site was determined as 0.018m^3/hr (18L/hr).

The test loop supernate flow set the size of the holding tank and the initial volume of solution needed for a finite run without the provisions for diluting the stream or for recycle. Determination of the size of the heat exchanges needed to obtain a finite temperature drop of the surrogate stream was accomplished by relating the heat drop deemed necessary to produce a plug. These experiments are described below. In summary, the chosen surrogate was clear at 55˚C and formed a gel at 40˚C. Lower gel points were observed with dilution of the sample. A temperature drop of 25˚C was desired.

The exchangers were sized by equating the heat to be extracted from the test solution with the heat capacity of the exchangers. A water jacket diameter of 2.54 cm and length of 45.37 cm was determined.

Components for the system were then obtained and configured as shown in Figure 14. The thermocouples, the stainless steel channel, the pressure transducers, and the surrogate/hot water flow meter were selected to minimize corrosion. Sampling ports were located at different points along the flow train. The simulated waste composition was prepared in the inlet tank at an elevated temperature of 70˚C and then cooled down to 55˚C. The outer bodies of the heat exchanger were constructed from PVC pipe. A booster pump, not shown, was used to increase the delivery of water from the tap.

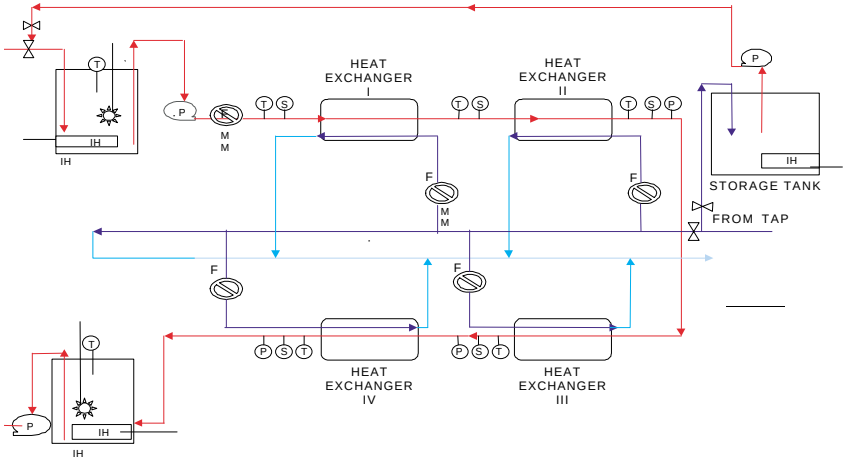

FIGURE 14. Block diagram of the laboratory-scale salt well pumping apparatus designations are as follows: p, pressure transducer; t, thermocouple; f, flow meter; ih, immersion heater; s, strain gauge or sampling port. Red lines correspond to the flow of the surrogate and/or dilution water; blue lines indicate cooling water.

Flow rates from 0.3 to 1.6 gpm, selectable for each exchanger, could be obtained for each module. Shutting off three of the exchangers allowed a flow rate as high as 3 gpm through the remaining shell. Provisions for recycling the surrogate sample to the inlet tank prior to the solution entering the channel, in the case of a downstream plug, and at the end of the channel in the event a plug did not form was included in the design. The inlet stream recycle aided in continually mixing the tank contents.

In the event of plug formation the sample line could be drained at the sample port and hot water could be added at the pump head in an attempt to unblock the channel. The location of the sample ports also allowed investigation on the effect of the amount of flush water. Specifically, following operation of the apparatus with the given stream, the remaining contents in the line were drained and water added at the pump head. Collecting additional samples during the flushing process

allowed for an indication of the ionic species remaining in the channel following the experiment.

All of the thermocouples, pressure transducers, and strain gauges were interfaced to a data acquisition and control system. At present all of the controls for the system are manual; provisions for automated control may be added in the future.

Experiments to determine heat exchanger performance and to obtain the friction factor of the loop were performed. The fluid for the tube was water and flow rates to the exchangers could be set from 0.3 gpm to 1.8 gpm with all exchangers active. The flexibility of the experimental apparatus also permitted the use of a cooling bath for one of the exchangers.

The temperature at which the gel forms (~40˚C) indicates that some care will have to be taken in the initial flow experiments. Figure 15 is a plot of the temperatures at various locations of the flow train as a function of time while the flow rate to the exchanges was 0gpm. In this case water was already present in the exchangers and the temperatures represent passive cooling of the hot water tube fluid.

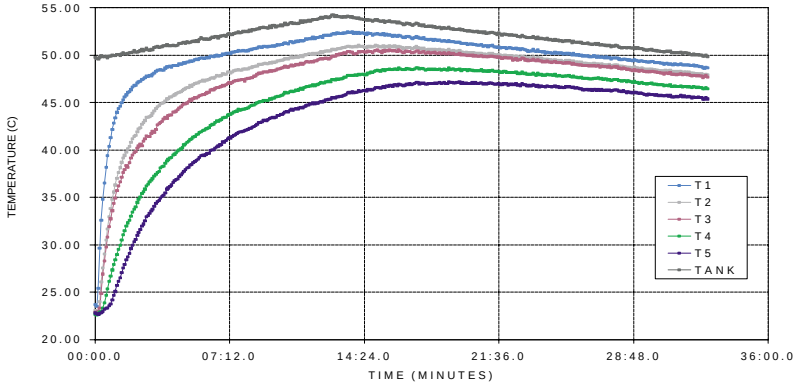

FIGURE 15. Flow stream temperatures with no flow to the heat exchangers.

The variation in T1 corresponds to the thermal cycling of the immersion heater in the inlet tank. The data indicate that a temperature of around 45˚C can be obtained throughout the entire flow loop with no cooling water flow.

Operation of all for heat exchangers with 0.3 gpm cooling water flow rate is given in Figure 16.

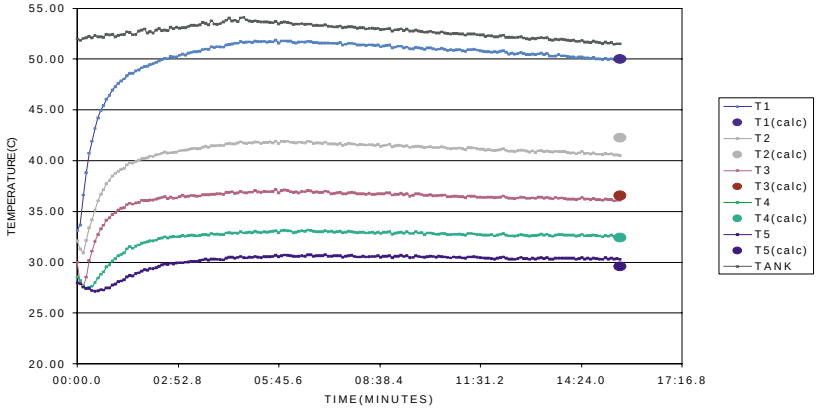

FIGURE 16. Channel fluid temperatures with all four heat exchangers operated at 0.3 gpm.

The data points in the figure correspond to the temperatures predicted by the heat transfer calculations for an input temperature of 50˚C and the same cooling water flow rates. The maximum difference between the calculated and measured temperatures was for thermocouple 2 and amounted to 1.8˚C and the standard deviation for all readings was 0.6˚C indicating that the model accurately accounts for heat transfer in the flow loop.

Flows to the exchangers greater than 0.3 gpm did not produce additional significant cooling.

The test loop was calibrated using water. Pressure drops recorded by the transducers (Fig. 14) are provided in Figure 17 for water flowing through the channel at the Reynolds number of 180. The transducers are approximately equally spaced along the channel and the differences between transducers 1 and 2, and between 2 and 3 are, within error, the same.

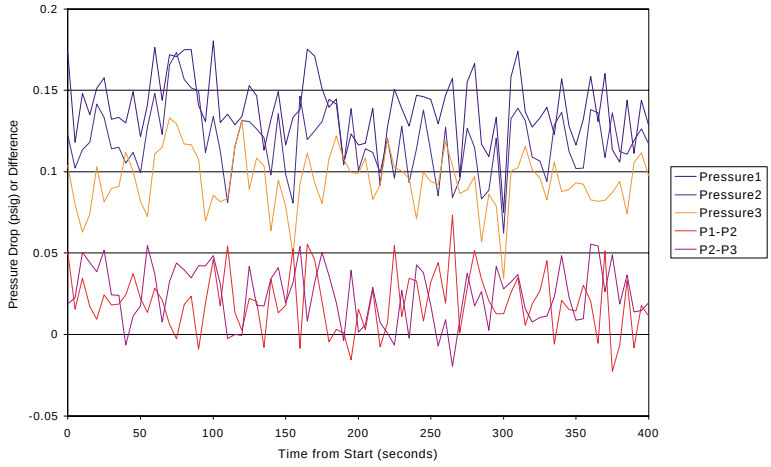

FIGURE 17. Pressures measured in the flow loop during pumping of water.

241-SX-104 Surrogate Screening

The SX-104 surrogate recipe was developed by R. Hunt at ORNL and was largely based upon previous studies of the tank supernate performed at Hanford.[32-34] Anion concentrations are given in Table 6. Sodium was the cation in all cases. Samples 5 and 8 were developed in the DIAL laboratories following the initial evaluation of the ORNL surrogate.

Previous work with the actual SX-104 supernate stream by Herting, revealed that a gel, based on sodium phosphate dodecahydrate ($Na_3PO_4 \cdot 12H_2O \cdot 0.25NaOH$), formed upon cooling the liquid to

22˚C.[32] Some dark gray solids were observed with the original SX-104 samples, which were removed by centrifugation prior to the cooling tests.

TABLE 6. Tank 241-SX-104 supernate surrogate compositions.

ANION	ORNL[(a)]	SAMPLE 5	SAMPLE 8
Aluminate	1	1	1
Nitrate	7	7	7
Hydroxide	2	2	2
Phosphate	0.2	0.3	0.3
Carbonate	0.4	0.4	0.1

Different plug formation methods are clearly possible when transferring the different Hanford waste streams. For slurries, particle deposition and subsequent build-up is anticipated at velocities smaller than the critical velocity. Plug formation in salt well pumping may occur in this manner but it is also likely that gels could form leading to a plug. The driving force for the later mechanism is a reduction in stream temperature.

The ORNL surrogate (and Samples 5 and 8) was prepared at a temperature of 70˚C in the laboratory and then examined visually and with the PLM as a function of temperature. On cooling to 40˚C the ORNL composition (Rodney 2, Fig. 18) formed a gel along with some loose solids, observable in the bottom of the glass tube. Changes to the original recipe, Table 6, were made in an attempt to reduce the amount of loose solids, thereby providing the potential for produce a plug based on gel formation only. Sample 5 provided a large amount of solids whereas the formulation for Sample 8 yielded gel only. PLM images for the ORNL and Sample 8 surrogates are given in Figures 19 and 20.

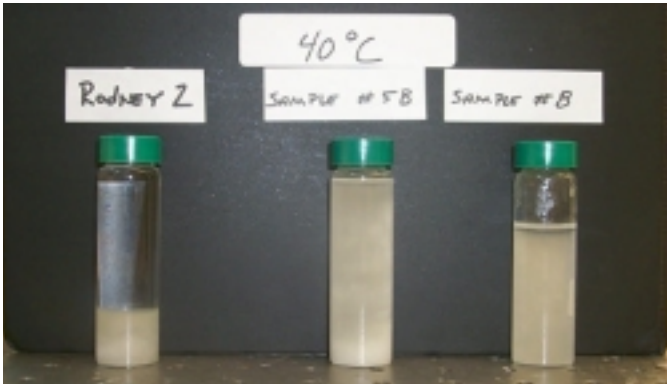

FIGURE 18. Visual observation of the SX-104 surrogates at 40˚C.

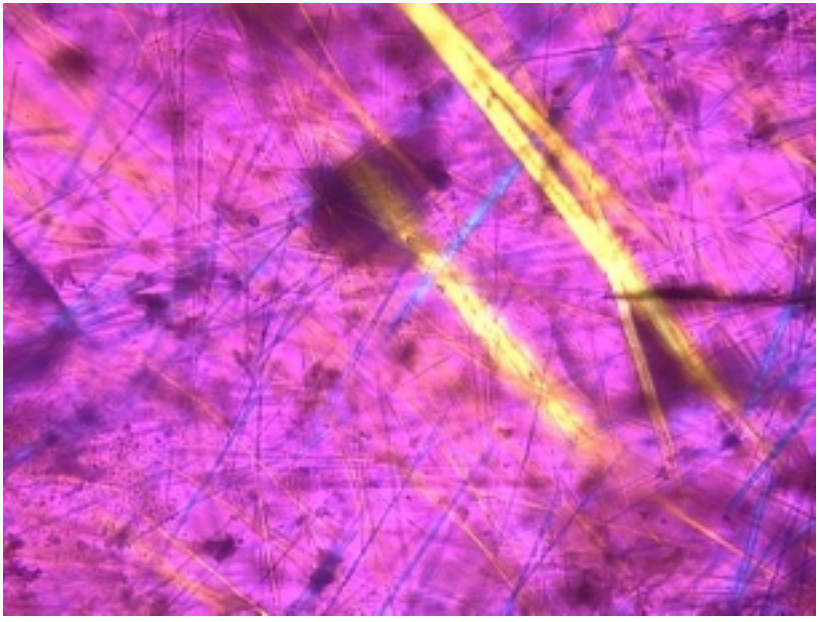

FIGURE 19. Polarized light microscope image of the ORNL surrogate, 40˚C 100x magnification.

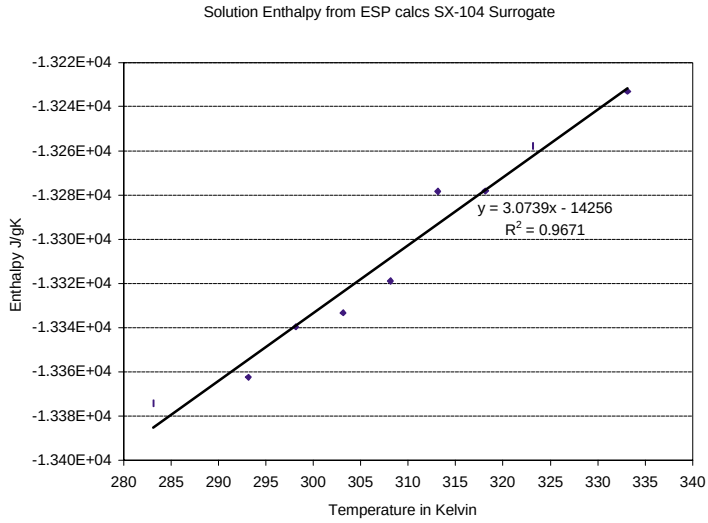

FIGURE 20. PLM image of Sample 8, 40˚C, 100x magnification.

The long cylinders or rods observed in both images are crystals from $Na_3PO_4 \cdot 12H_2O \cdot 0.25NaOH$. The solids in Figure 19 have been identified as gibbsite ($AlOH_3$). The PLM results are consistent with the solids fraction observed in the photograph (Fig. 18). The crystals in the PLM image for Sample 8 at 25˚C (not shown) consisted of the sodium phosphate dodecahydrate and sodium nitrate. The PLM images for Sample 8 are similar to the images of the actual SX-104 supernate as reported by Herting.[32] The main difference between the waste stream supernate and Sample 8 is that gel formation was observed for Sample 8 consistently at 40 ± 1˚C, whereas the actual waste stream liquid was found to form a network at 22˚C.

Decreasing the temperature from 40 to 25˚C resulted in gels of more rigidity. At 40˚C, Sample 8 contains a small amount of liquid on top of the gel, Figure 18. At 25˚C, the sample vial could be inverted and vigorously shake without flow.

ESP Calculations Supporting the Laboratory Salt Well Pumping Experiments

The compositions in Table 6 provide a means to study plug formation during salt well pumping if only a gel forms or if a gel is formed along with various amounts of loose solids. ESP calculations (version 6.2) were carried out to provide additional information on surrogate chemistry and stream properties, such as enthalpies, solid-liquid partitioning, and liquid viscosities that are of interest in the actual pumping experiments. The chemistry model was constructed from the sodium species of Table 6. The Lab, TRONA, and Public Databases were employed. Initially the ORNL and Sample 8 surrogates were evaluated as a function of temperature. The Sample 8 surrogate was then evaluated at different dilutions. These later experiments were then compared to experimental observations similar to Figure 18.

The solids distributions for the Sample 8 surrogate at the different temperatures are collected in Table 7.

TABLE 7. Solids compositions and phase information for Sample 8 SX-104 surrogate.

Temperature C	15.00	20.00	25.00	30.00	35.00
Solids g					
$Al(OH)^3$	31.37	25.77	19.16	11.42	3.51
$NaNO^3$	135.33	103.56	68.82	30.50	0.00
NaPHOH $12H_20$	84.69	80.45	72.67	58.92	37.15
$Na^3PO_4{\cdot}8H_20$	0.00	0.00	0.00	0.00	0.00
Total wt in g	251.39	209.77	160.64	100.84	40.66
Volume L	0.13	0.11	0.08	0.05	0.02
Density g/L	2008.02	1975.56	1929.41	1846.82	1667.56
% PO_4 Solids/Total	33.69	38.35	45.24	58.43	91.37

TABLE 7. Solids compositions and phase information for Sample 8 SX-104 surrogate.

Temperature C	40.00	42.00	43.00	50.00	
Solids g					
$Al(OH)^3$	0.00	0.00	0.00	0.00	
$NaNO_3$	0.00	0.00	0.00	0.00	
NaPHOH $12H_20$	9.35	0.00	0.00	0.00	
$Na_3PO_4{\cdot}8H_20$	0.00	9.26	1.25	0.00	
Total wt in g	9.35	9.26	1.25	0.00	
Volume L	0.01	0.01	0.00	0.00	
Density g/L	1619.96	1619.96	1619.96	0.00	
% PO_4 Solids/Total	100.00	100.00	100.00	0.00	

At temperatures above 41˚C the only solid predicted by ESP is sodium phosphate octahydrate. Attempts to observe the corresponding crystal with the PLM were unsuccessful. The particle size is apparently smaller than that dimension observable with the highest effective magnification of the microscope, 400x.

At an approximate temperature of 40˚C the octahydrate crystal is partitioned to the dodecahydrate which comprises 100% of the solids in the system at that temperature. Gibsite forms on cooling the composition to 35˚C and at lower temperatures the model predicts the formation of $NaNO_{3(s)}$. The model correctly predicts the crystal observed in the PLM images; however, the fact that the solids form an ordered network cannot be predicted by the code.

Totals for the Sample 8 surrogate stream are given in Table 8. The calculated density at 50˚C is above the criteria for waste transfers of 1.35 g/L (for liquids with less than 30% solids) and below the waste compatibility limit of 1.41 g/L.[31] The total stream density increases

with reducing temperature owing to the additional partitioning into the solid phase.

TABLE 8. ESP predictions for Sample 8 at different temperatures.

Temperature C	**15.00**	**20.00**	**25.00**	**30.00**
Mass g	1373.53	1373.53	1373.53	1373.53
Volume L	0.96	0.96	0.97	0.97
Density g/L	1437.78	1429.97	1420.86	1410.24
% Solids by Wt.	18.30	15.27	11.70	7.34
% Solids by Vol.	13.11	11.05	8.61	5.61
% Water by Wt.	49.22	49.39	49.70	50.26
Temperature C	**40.00**	**42.00**	**43.00**	**50.00**
Mass g	1373.53	1373.53	1373.52	1373.53
Volume L	0.99	0.99	0.99	1.00
Density g/L	1388.26	1384.30	1383.35	1373.53
% Solids by Wt.	0.68	0.67	0.09	0.00
% Solids by Vol.	0.58	0.58	0.08	0.00
% Water by Wt.	52.26	52.32	52.59	52.64

At the gel temperature of 40˚C, Figure 18, the model predicts the formation of ~9 g of solid sodium phosphate dodecahydrate per L of solution.

The heat capacity is a critical value for determining the heat transfer characteristics of a given process. As part of the standard output from ESP stream enthalpies and a total solution enthalpy are reported. Figure 21 is a plot of stream enthalpy against absolute temperature (K), the slope of the line; dH/dT is, by definition Cp.

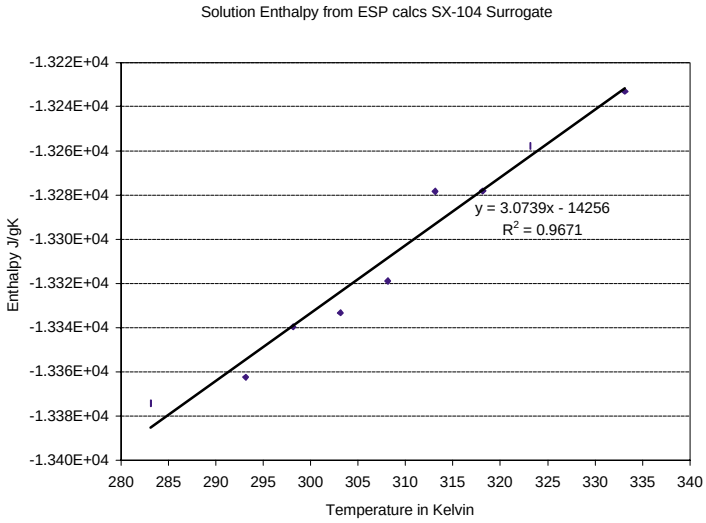

FIGURE 21. Prediction of the heat capacity for Sample 8 based on ESP.

ESP Simulations and Experimental Results for Dilution of SX-104 Surrogate Sample 8

Determination of the amount of dilution water needed to safely transfer salt well liquor will depend on the composition of the supernate and the solid-liquid partitioning at different temperatures. Water is used for both dilution and line flushing and both operations result in an increase in waste volume. From evaluation of the conditions that lead to the SX-104 plug it appears that the operators were processing the liquid with no dilution water, stopped the transfer for a while, and on re-start developed a plug in an unheated jumper.[31] The plug was remediated using hot water. Dilution water was subsequently injected at the pump head.

The technical basis for dilution and line flushing operations during salt well pumping is not well established and, are in fact, major benefits expected from this work. It has been noted that diluting the salt well liquor 1:1 has worked in preventing plugs.[31] Flushing is

accomplished using one line volume of water and has occurred on different schedules. Nominally, the line is flushed whenever the jet pump is down for longer than two hours. Flushing has been performed every week and is currently done every 21 days. The frequency of flushing as well as the extent of dilution water added will depend on the stream composition and the waste routing.

The ESP model was used to calculate the effect of dilution water on the surrogate stream. These results correspond to dilutions of 25, 50, 75, and 100% by volume and details will be reported later. A 100 cc volume of the sample was made in the laboratory at elevated temperature (70˚C and until clear) then distributed to five different vials and subsequently diluted.

Gels were observed for the 1:0.25 and 1:0.5 dilutions at 30˚C. On cooling to 25˚C a gel was observed for the 1:0.75 sample. A gel was not found for the sample diluted 1:1.

The samples were subsequently placed in the oven at 70˚C overnight and then re-examined. Gibbsite ($AlOH_3$) was observed to form on the bottom of the test tubes. Upon cooling only the baseline Sample 8 composition without dilution (Table 6) formed a gel. This indicates that a re-partitioning of the samples occurred following the precipitation of the $AlOH_3$.

Experiments on Plug Formation

An 18 L batch of the surrogate (Sample 8) was prepared in the holding tank. The sample channel was pre-heated with hot water from the water dilution tank to a temperature of about 60˚C. The channel was then drained at the surrogate flow started at a rate of 4.8 gph. The liquid was allowed to flow in the channel and then to the receiving tank where it was collected prior to transfer back to the holding tank. Temperatures were allowed to stabilize with no forced cooling and then the water to the fourth heat exchanger (see Fig. 14) was started at

0.33 gpm for 45 seconds. Figure 22 illustrates the holding tank and thermocouple temperatures and the response of the pressure transducers.

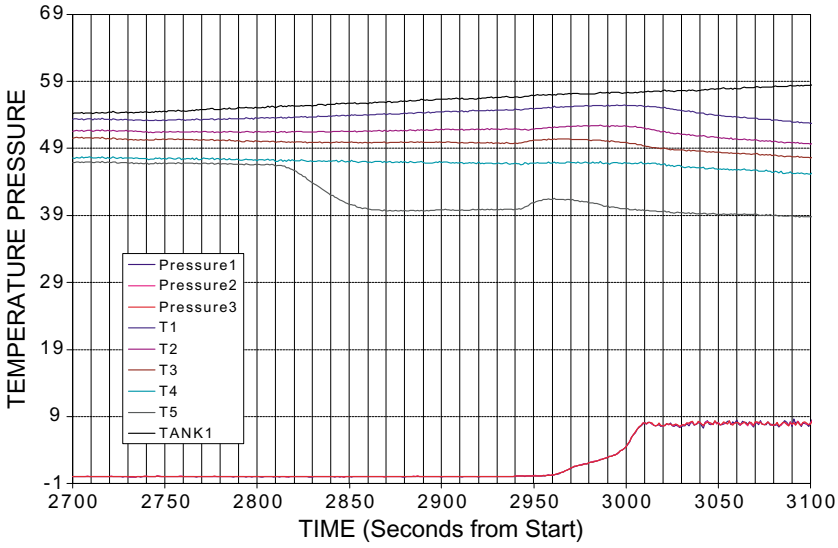

FIGURE 22. Flow loop thermocouple and pressure transducer traces during one of the test runs.

Following application of cooling at heat exchanger 4 the temperature of the surrogate stream dropped from ca. 46 to 39˚C. Average pressures until around 2950 seconds into the run were constant. At 2960 seconds an increase in the temperature of the fluid at T5 was observed along with an increase in pressure. At a time of 3010 seconds the pressure maximized indicating plug formation.

The exotherm observed is repeatable and visual observations of the flow obtained by routing the solution to a clear tube attached to the last sampling port illustrated the particle growth process. Initially, the solution remained clear, followed by the occurrence (at lower temperatures) of individual phosphate rods. Thereafter the solution

became turbid and this was followed by gel formation. Additional experiments are needed to determine the full effects of temperature, flow rate, dilution, and line flushing.

Conclusions

Results have been described for the experimental portion of the Prevention of Solids Formation Program. An experimental salt well pumping flow loop was designed, fabricated, and tested. Experiments on a surrogate waste stream for Hanford tank 241-SX-104 were conducted on the laboratory bench and in the facility. ESP calculations were shown to predict the proper solids involved in the gelation process but were not capable of predicting the formation of the three-dimensional gel structure. Preliminary experiments with the surrogate in the salt well pumping apparatus indicated that gelation can be rapid but was characterized by an exotherm corresponding to formation of the trisodium phosphate dodecahydrate crystals and an associated increase in pressure. A maximum in the pressure was observed indicating the formation of a plug. The work support the use of ESP in characterizing the solid liquid equilibria and will allow future studies relating flow, temperature excursions, dilution, and operations at the site.

Work Planned

The companion portion of this project involves the development of an engineering model that will describe slurry transfers and salt well pumping operations at Hanford. Work on these tasks has begun and preliminary computational fluid dynamic simulations have been performed and reported for two-phase flows.[35] This work will be described in the next report along with the experimental studies currently underway.

References

31. D.A. Reynolds. May 2000. *Status of Waste Transfers, Criteria, and Plans.* Presented at the Saltcake Dissolution and Feed Stability Workshop, Richland WA.

32. D.L. Herting. 1998. *Tank 241-SX-104 Dilution Testing, Interim Report.* Internal Memo 8C510-PC98-024, Numatec Hanford Corporation, Richland, WA.

33. F.H. Steen. 1999. *Ammonia Analysis Results for the Final Report for Tank 241-SX-104.* Memo WMH-9852843, Numatec Hanford Corporation, Richland, WA.

34. F.H. Steen. 1999. *Analysis Results for the Final Report for Tank 241-SX-104.* Memo WMH-9856353, Numatec Hanford Corporation, Richland, WA.

35. J.S. Lindner and H. Al-Habbash. May 2000. *Saltwell Pumping/Pipeline Plugging* and *Model Development for the Waste Transfers.* Presented at the Saltcake Dissolution and Feed Stability Workshop, Richland WA.

TASK 4

*Diagnostic Field Applications Coordination and Testing Support (**DFACTS**)*

Introduction

As part of the DIAL/DOE Cooperative Agreement, a diagnostic field applications, coordination, and testing support (DFACTS) program has been initiated. The DFACTS program addresses the need for on-site measurement of various performance parameters employing DIAL's field applications measurement systems. This aids in the rapid demonstration and implementation of modern fieldable diagnostic methods by providing on-site measurements with DIAL's diagnostic systems and by coordinating and supporting demonstration field tests of instrumentation systems from diagnostic developers within the private sector. Moreover, these on-site measurements provide direct testing support to the DOE complex. This not only provides information for evaluating the applicability of measurement techniques, but also provides a significant add-on-value to the testing efforts being carried out across the DOE complex. This testing support is a major element and advantage of the plan. One major advantage of DIAL involvement is that, because the measurements are made by an independent third party, they also carry more weight in convincing stakeholders that the particular process is effective.

Work Accomplished

To implement the DFACTS effort, money has been budgeted to support the program. Over the last three months, we have been making every effort to advertise the program and DIAL's capabilities. In particular, we have pointed out that DIAL can provide state-of-the-art measurement systems and expertise to support various development applications from laboratory-scale to large scale test facilities. Moreover, the diagnostic methods and capabilities of DIAL can, in general, provide:

- real time measurement of process/performance parameters;
- evaluation/characterization of high temperature gas flows;
- process characterization/improved understanding;
- validation data for model development;
- process monitors/control;
- environmental monitoring, CEMs;
- EPA reference methods;
- analytical laboratory;
- diagnostic development;
- engineering development/solutions to technical problems; and,
- in-house testing/cost effective, flexible, non-biased.

A number of areas of interest have been identified where DFACTS could contribute. In particular,

- particulate CEM testing;
- mercury CEM testing;
- Hg CEM calibration standards; and,
- HEPA filter testing.

Work Planned

HEPA filter testing may be implemented first. DIAL is presently working with the DOE/EPA Technical Working Group on HEPA filter performance and monitoring. The performance of these filters is of critical importance to DOE since they provide the final physical barrier to the release of particulate matter to the atmosphere.

The effect on the performance of such quantities as moisture, temperature, over pressure, breach, shelf life is particularly important, as well as the effect of off-gas character on long-term performance. To be able to provide real time filter performance, and to provide system feedback control, the ability to measure the particulate character before and after the filter is needed. Understanding the role of particle size range and detectability is important. To this end, an effort to evaluate methods for particulate monitoring will be initiated. Results from this filter testing program can be provided in the field via the DFACTS program.